UNIVERSITETET I AGDER

Modelling heat diffusion in concrete structures during a tunnel fire, to investigate structural safety

Annikken de Lange

SUPERVISORS
Rein Terje Thorstensen, UiA
Ian Willoughby, Bane NOR

University of Agder, [2019]
Faculty of Engineering and science
Department of Engineering Sciences

Obligatorisk egenerklæring/gruppeerklæring[1]

Den enkelte student er selv ansvarlig for å sette seg inn i hva som er lovlige hjelpemidler, retningslinjer for bruk av disse og regler om kildebruk. Erklæringen skal bevisstgjøre studentene på deres ansvar og hvilke konsekvenser fusk kan medføre. Manglende erklæring fritar ikke studentene fra sitt ansvar.

1.	Jeg/vi erklærer herved at min/vår besvarelse er mitt/vårt eget arbeid, og at jeg/vi ikke har brukt andre kilder eller har mottatt annen hjelp enn det som er nevnt i besvarelsen.	☒
2.	Jeg/vi erklærer videre at denne besvarelsen: - ikke har vært brukt til annen eksamen ved annen avdeling/universitet/høgskole innenlands eller utenlands. - ikke refererer til andres arbeid uten at det er oppgitt. - ikke refererer til eget tidligere arbeid uten at det er oppgitt. - har alle referansene oppgitt i litteraturlisten. - ikke er en kopi, duplikat eller avskrift av andres arbeid eller besvarelse.	☒
3.	Jeg/vi er kjent med at brudd på ovennevnte er å betrakte som fusk og kan medføre annullering av eksamen og utestengelse fra universiteter og høgskoler i Norge, jf. Universitets- og høgskoleloven §§4-7 og 4-8 og Forskrift om eksamen §§ 31.	☒
4.	Jeg/vi er kjent med at alle innleverte oppgaver kan bli plagiatkontrollert.	☒
5.	Jeg/vi er kjent med at Universitetet i Agder vil behandle alle saker hvor det forligger mistanke om fusk etter høgskolens retningslinjer for behandling av saker om fusk.	☒
6.	Jeg/vi har satt oss inn i regler og retningslinjer i bruk av kilder og referanser på biblioteket sine nettsider.	☒

[1] Only given in Norwegian from the University

Publiseringsavtale[2]

Fullmakt til elektronisk publisering av oppgaven

Forfatter(ne) har opphavsrett til oppgaven. Det betyr blant annet enerett til å gjøre verket tilgjengelig for allmennheten (Åndsverkloven. §2).
Alle oppgaver som fyller kriteriene vil bli registrert og publisert i Brage Aura og på UiA sine nettsider med forfatter(ne)s godkjennelse.

Oppgaver som er unntatt offentlighet eller tausehetsbelagt/konfidensiell vil ikke bli publisert.

Jeg/vi gir herved Universitetet i Agder en vederlagsfri rett til å gjøre oppgaven tilgjengelig for elektronisk publisering: ☒JA ☐NEI

Er oppgaven båndlagt (konfidensiell)? ☐JA ☒NEI
(Båndleggingsavtale må fylles ut)
- Hvis ja:
Kan oppgaven publiseres når båndleggingsperioden er over? ☐JA ☐NEI

Er oppgaven unntatt offentlighet? ☐JA ☒NEI
(inneholder taushetsbelagt informasjon. Jfr. Offl. §13/Fvl. §13)

[2] Only given in Norwegian from the University

1. Preface

During the preliminary report to this master's thesis, I experienced even greater interest in fire safety design and looked forward to immersing myself in the subject. This has been a very educational period where I have gained valuable insight concerning fire simulations and the heat diffusion that develops in concrete structures during a fire.

This is my final report ending a five-year education. I would like to thank my supervisor Rein Terje Thorstensen at UiA for guidance along not only for this master's thesis but also during the period for my preliminary report in advance of this master's thesis and during the period for my bachelor report. I would like to thank my supervisor Ian Willoughby at Bane NOR for guidance through both the preliminary report and this master's thesis. I would also thank Katalin Vertes and Kameran Aziz for their time and help within the software.

In the end, I would like to direct a special thanks to Svend Oddvar Åsrud, for invaluable help with the software ANSYS and fire simulations. Without your help, I would probably still be writing on this master's thesis.

2. Summary

This is my master's thesis for my master's degree in civil engineering. In this study, the heat diffusion in concrete structures during a tunnel fire is investigated. The available literature on the heat diffusion of the ISO 834, EUREKA 60, 90 and 120, HC and RWS fire curve have been investigated and compared. The fire curves are also modelled in the software ANSYS, where different approaches have been simulated, and temperature profiles have been established. The different analyses have been developed and performed from a literature study, watching tutorials online and through meetings with experts.

The importance of including all three heat transfer processes emerged through the study. The 1D-model based on elements with properties for conduction, convection, and radiation corresponded well with the temperature profiles presented in Eurocode 2, which indicates that the model is adequate for comparison. The material properties of concrete are considered, and the fire is simulated as a gas-temperature load.

The different fire curves seem to influence the heat diffusion by the maximum achieved temperature, the steepness of the curve, the duration of the fire, and the cooling stage. The RWS fire curve is the fire curve that achieved the highest heat diffusion in the concrete. If the ISO 834 fire curve is assumed for a fire duration of 240 minutes, the heat diffusion will be higher than the heat diffusion of the EUREKA 120 fire curve.

3. Table of contents

4. Figures

5. Tables

6. Introduction

This master´s thesis is written spring 2019 at the University of Agder as a prolongation of the preliminary report written autumn 2018. The preliminary report revolved the existing procedures concerning the performance of a fire design of load-bearing concrete structures. From the preliminary report, it emerged that the most used fire curves in Norway are the ISO 834, EUREKA (RABT/ZTV train), HC, and RWS. It also emerged that the ISO 834 fire curve is best suited for buildings and not compatible with a fire inside a tunnel.

Bane NOR, the Norwegian enterprise responsible for the national infrastructure, recommends the use of the EUREKA fire curve when dimensioning load-bearing concrete tunnels for fire. However, the regulations, TSI SRT[3], open for other fire curves to be used. Bane NOR have experienced that consultants have ignored the recommendation of using the EUREKA fire curve and rather used the ISO 834 fire curve with a prolonged time duration. Hence, it is interesting to investigate how the different fire curves will influence the heat diffusion in the concrete when altering the fire durations.

[3] TSI SRT – technical Specification for Interoperability Safety in Railway Tunnels

7. Societal perspective

Industrialization has become a more and more popular term within the industry. The use of digital tools will make the industry more effective, but this skill seems to be neglected or forgotten by educational institutions [1].

SINTEF [2] has compiled five dimensions of industrialization; organization, scale, variation, automation, and the use of technology. The five dimensions presented by SINTEF are shown in figure 7-1 below.

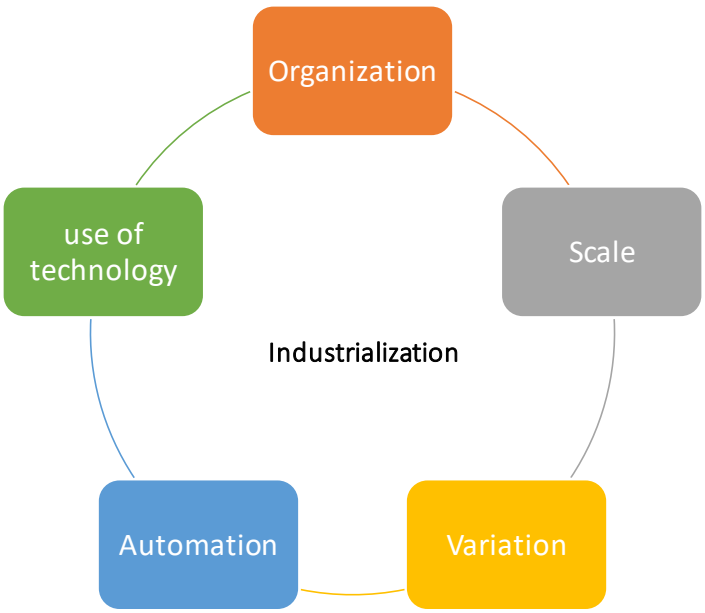

Figure 7-1 The five dimensions freely translated and rendered from [2]

The use of technology as a step for a more industrialized industry will involve a digitized process [3], which means that by implementing finite element analysis programs in the engineering, the industry is also moving towards industrialization.

A computer analysis will often be preferred if the problems have a high range of complexity. These problems are often very time-consuming or maybe even impossible to perform by hand calculations and will, therefore, be suited for a computer analysis. However, there is a high cost associated with this type of analysis, which makes the use of this method not beneficial for solving simple problems [4].

8. Theory

The theory chapter is divided into different sub-chapters to ease the reading. Starting with an introduction to different types of tunnels and ending with a description of the used modelling techniques. The concrete behavior during fire, the heat transfer processes and the different fire scenarios are also addressed here.

8.1. Surrounding Environment

Tunnels are often categorized after the surrounding environments soil conditions. It is normal to distinguish between tunnels that go through rocks and tunnels that go through soils when a tunnel is being constructed [5].

The tunnels that go through soil is often referred to as a load-bearing tunnel because the concrete itself is the load-bearing element. Oddernestunnelen in Kristiansand is an example of a tunnel of this kind. The tunnel is showed in figure 8-1 below. Tunnels where the rock itself is the load-bearing element is often only referred to as a tunnel. The Trøde-Bråhei tunnel in Lillesand is an example of a tunnel of this kind. The tunnel is showed in figure 8.2 below.

Figure 8-1 Photo of a load-bearing concrete tunnel, Oddernestunnelen in Kristiansand [6]

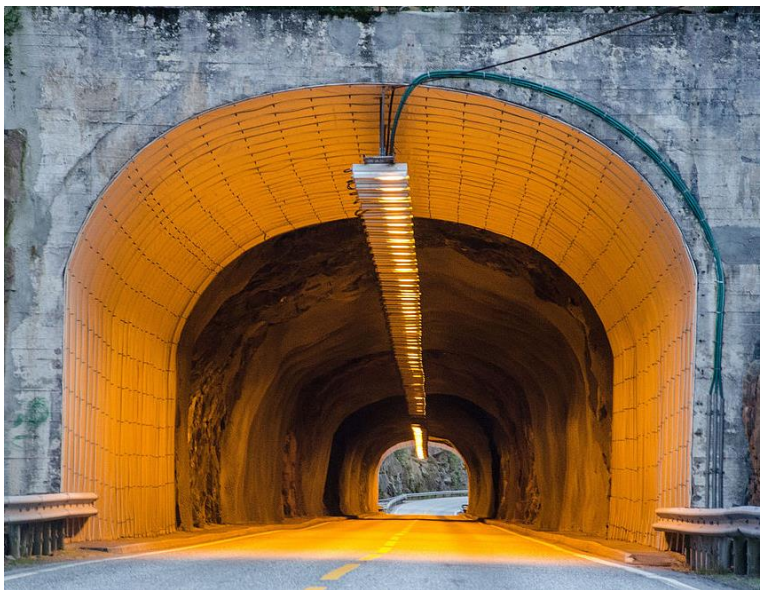

Figure 8-2 Photo of a rock tunnel, Trøde-Bråhei in Lillesand [7]

8.2. The behavior of concrete when exposed to elevated temperatures

Different concrete types behave similarly at elevated temperatures, such as in a fire [8]. When concrete is exposed to fire, there are generally two problems. These two problems are concrete spalling and deterioration of the material properties. The concrete spalling will lead to a reduction of the concrete cross-section and possible exposure of the reinforcing steel, while the deterioration of the material properties will decrease the compressive and tensile strength of the concrete [9]. The probability of explosive spalling to occur increase with increased heating rate, with applied loads, higher concrete strength, and thermal expansion [10]. The addition of polypropylene fibers reduces the chance of spalling remarkably, and 0.5-2 kg of polypropylene fibers per m^3 concrete is enough to enhance the fire resistance [11].

The dehydration of the cement in the concrete will lead to a significant decrease in the materials stiffness and strength [12]. When it comes to strength loss, the critical temperature of siliceous concrete is 300°C [9]. Similarly, the reinforcing steel also loses its strength and stiffness when exposed to elevated temperatures [12]. The highest temperatures is normally obtained close to the ceiling [13].

The thermal properties of the concrete material need to be known to be able to calculate the temperature development in the concrete [8]. The loss of strength and stiffness in the reinforcing steel at elevated temperatures can be seen in table 8-1 below.

Table 8-1 Stress-strain relationship for hot rolled reinforcing steel at elevated temperatures [14]

Steel temperature [°C]	The stress-strain relationship for hot rolled reinforcing steel
20	1
100	1
200	1
300	1
400	1
500	0.78
600	0.47
700	0.23
800	0.11
900	0.06
1000	0.04
1100	0.02
1200	0

Although reinforced concrete structures with catastrophic failures in the fire are seldom, it happens. When it happens, it rarely happens because of the loss of strength of the materials. This happens mostly because of the inability of the other parts of the structure to absorb the imposed thermal deformations. Thus, shear or buckling failures of the columns or walls can occur [8].

Structural failure normally only occurs when the reinforcing steel achieves a temperature that results in loss of strength. A concrete structure exposed to fire might have structural damage, even if there is no visible damage to the structure. If a reinforced concrete slab is exposed to fire, and the strength of the reinforcing steel is lost, there will be bending or tensile strength failure [15]. Because steels with low carbon contents will exhibit blue brittleness between temperatures of 200-300°C, the recommendations are often that the reinforcing steel is protected to temperatures above this [15].

For normal weight concrete, the compressive strength is normally within the range of 20 to 50 MPa, and with a density of approximately 2300kg/m^3. Reinforced concrete structures depend on the concrete cover to protect the steel reinforcement from the exposure of elevated temperatures in a fire. The concrete cover is the concrete outside of the reinforcing steel and is measured as the distance between the surface and the reinforcing steel for durability considerations. For most of the engineering calculations, the distance is measured from the surface and to the center of the main reinforcing bars [8].

According to Fletcher et al. [15], the behavior of concrete during a fire is not characterized well, where further research is necessary for almost every aspect of its field. They state that simple treatments are used to describe fire environments, such as simple time-temperature curves or homogenous temperatures. This does not give a realistic representation of real fires.

It is normal to assume that the heat transfer is a function of the thermal properties of the concrete alone when the thermal calculations are being performed. Because most of the reinforcing steel is placed parallel to the fire-exposed surfaces, it is assumed that the thermal conductivity of the steel is neglectable. The temperature of the reinforcing steel is, therefore, assumed to be the same as the surrounding concrete [8].

The properties of the materials will change with time. Generally, materials will get softer when heated and become more brittle when cooled. Most materials will also respond to heat and cooling by respectively expand and contract. Most materials also seem to conduct heat better when they are warm [4].

8.3. Heat transfer

Due to the difference in temperature, a thermal energy transit occurs, which is referred to as heat transfer. This heat transfer can be divided into three different categories; convection, conduction, and radiation [16].

These three types of heat transfer can either occur individually or as a combined heat transfer process [17]. The heat transfer from a heat source to the tunnel lining should not be limited to a heat conduction analysis, but also include the heat convection and radiation [18]. Heat is transferred by both convection and conduction within the concrete when a concrete structure is exposed to fire [19]. Prediction of the thermal field within the structure during a tunnel fire is a complex phenomenon because of the combination of convective, conductive, and radiative heat transfer [20].

Because heat transfer from radiation is difficult to predict a combined heat transfer coefficient is often applied in a heat transfer analysis of a material exposed to elevated temperatures. This coefficient is defined as the convective heat transfer coefficient, but also includes the heat transfer by radiation [18].

The convective heat transfer coefficient differs from the thermal conductivity coefficient by not being a property of the material and because it varies remarkably with the heat flow configuration, thermodynamic fluid property, heat transfer surface, and flow area geometry and the heat transfer surface position [18].

Convection and radiation are the heat transfers that first takes place when there is a fire inside a tunnel. This is the heat transfer from the heat source to the concrete tunnel lining. When the temperature near the tunnel lining increases, conduction takes place [17].

Figure 8.3 below illustrates the three different heat transfer processes. Where radiation is the heat transfer from the fire, the convection is the heating of the water, and conduction is the heat transfer within the material. These three processes will be described further in the sub-chapters below the figure.

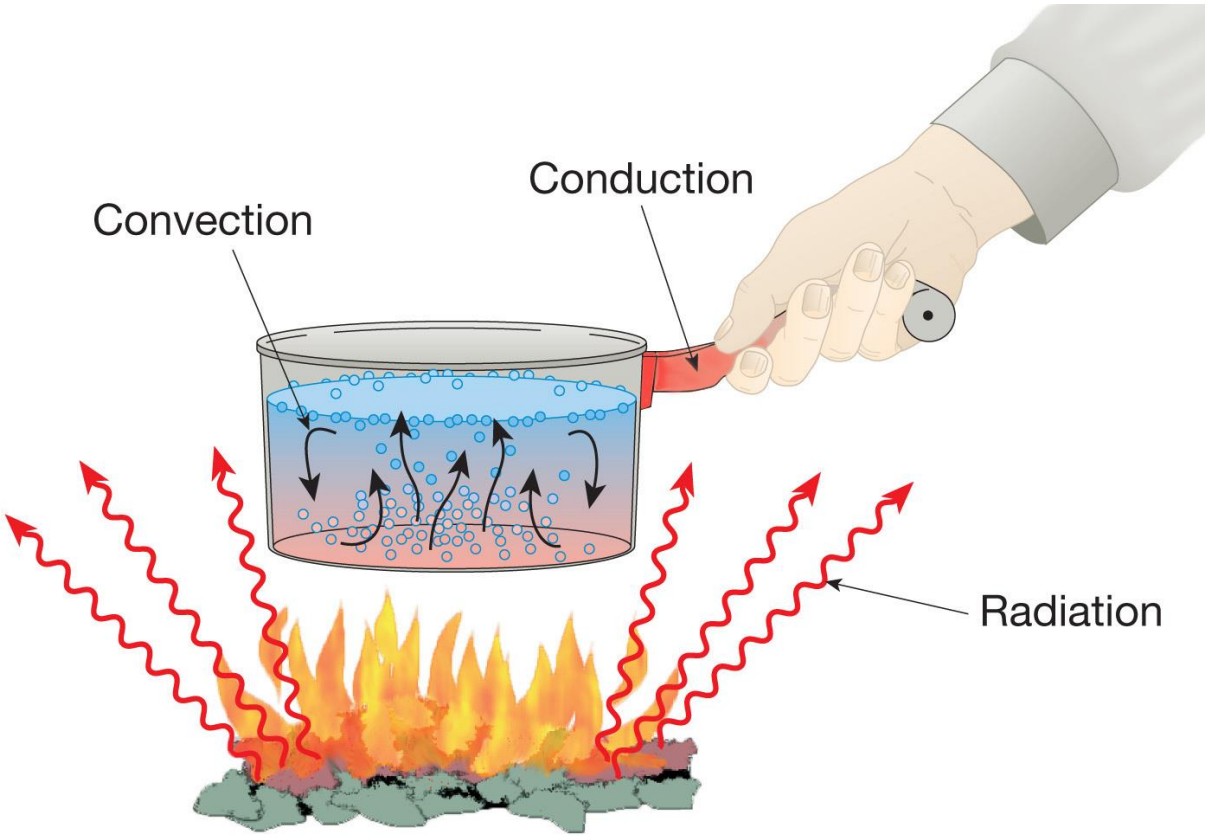

Figure 8-3 The three processes of heat transfer [21]

8.3.1. Convection

The heat transfer that will occur between the surface of a material and a moving liquid with different temperatures is called convection [16]. This is heat transfer, such as air or water [22].

According to the Eurocode [23], the coefficient of heat transfer by convection (α_c) is 25 (W/m^{2}K) for the ISO 834 fire curve and 50 (W/m^{2}K) for the hydrocarbon fire curve.

8.3.2. Conduction

The heat transfer that occurs through the material, which can be both solid and liquid, is termed conduction [16].

When considering heat transfer through conduction, the thermal conductivity value is important for concrete materials. This value is referred to as the k-value of the material [24]. A material with a large k-value is a material with good heat conductor properties, whereas a material with low conductor properties will have a k-value of smaller value [25]. When determining the thermal conductivity factor, the moisture content, temperature, type of aggregate, type of cementitious material, and the density of the concrete are important factors [24]. The thermal conductivity represents the materials ability to conduct heat [18].

Fourier's law is the rate equation for heat conduction. For a one-dimensional plane wall, with a temperature distribution T(x) the rate equation is expressed in equation **(8.1)** below [16];

$$q''_x = -k \frac{dT}{dx} \qquad (8.1)$$

Where:
q''_x is the heat flux (W/m^2)
k is the thermal conductivity (W/m × K)

This heat flow rate can be simplified as defined in equation **(8.2)** below, where the ratio between the cross-section and the length of the material is of importance in addition to the difference in temperature [25].

$$H = -k \frac{A}{l}(T_2 - T_1) \qquad (8.2)$$

Where:
H is the rate of the heat flow
A is the area of the cross-section
l is the length of the material
k is the thermal conductivity of the material
($T_2 - T_1$) is the temperature difference in the material

Heat transfer through conduction is a result of colliding molecules, where the transfer of energy from the more energetic to the less energetic occurs. Because higher temperatures are associated with

higher molecular energy, the heat transfer by conduction will occur in the direction of decreasing temperature. The minus sign in the equation originates from this explanation [16].

8.3.3. Radiation

Heat transfer through electromagnetic waves is referred to as radiation [16]. Indifference from convection and conduction thermal radiation does not need an intervening medium to carry it. It is emitted by a heated surface, in all directions, at the speed of light directly to the point of absorption [26]. In a tunnel fire where a solid material is exposed to heated air convection and radiation occur simultaneously [17].

Stefan-Boltzmann law states that the total radiant heat energy emitted from a surface proportional to the fourth power of its absolute temperature. The constant of the proportionality is called the Stefan Boltzmann constant, σ, and is equal to 5.670367 x 10^{-8} W/m^2K^4. This constant is used when the radiant heat energy is calculated [27]. The equation **(8.3)** below presents the radiant heat energy.

$$E = \sigma T^4 \qquad (8.3)$$

Where:
E is the radiant energy emitted from a unit area in one second
σ is the Stefan-Boltzmann constant
T is the absolute temperatures in Kelvin

Different surfaces absorb and radiate thermal radiation differently, but the surfaces that are good emitters are also good absorbers [26].

8.4. Fire scenario

According to the Eurocode [23], structural fire design should take these steps into consideration:

- Selection of the relevant fire design scenario, and the determination of the corresponding design fire
- Calculation of the temperature distribution within the structural parts
- Calculation of the mechanical behavior of the construction exposed to fire

Actions from fire exposure are classified as an accidental action, according to the Eurocode. Unless specified otherwise, it may be assumed that the design fire is given by the standard fire, where the national authorities specify requirements for the structural fire resistance. The calculation of the mechanical behavior, the mechanical analysis, shall have the same duration as the temperature analysis of the structural parts [23].

8.4.1. Prediction of thermal impact

The high temperatures that are encountered in fires inside tunnels can cause spalling and dehydration of the concrete material, which results in a reduction of the tunnel lining and structural instability of the tunnel. The high temperatures also impact the mechanical and thermal properties of the remaining structural part of the tunnel. Hence, to predict the potential fire-induced damage and

structural loss to the tunnel lining becomes important. This prediction is often based on a heat transfer analysis [18].

Nevertheless, it is important to know that this type of analysis only is valid if there is no structural loss due to spalling or dehydration. Because of this, the results from these tests will be underestimated [18]. The concrete must stay in place in order for the thermal calculations to be correct. If spalling occur, this will not be fulfilled. Therefore, the calculations should consider that some of the material will be lost due to spalling. This is often difficult because there is not a method for estimating the amount of spalled material [11].

A conventional thermo-mechanical coupled analysis for stability analysis of a fire-damaged structure does not consider the structural loss due to spalling [18].

Thermal actions are given by the **net heat flux** to the surface of the member[23]:

$$\dot{h}_{net} = \dot{h}_{net,c} + \dot{h}_{net,r} \quad [W/m^2] \tag{8.4}$$

Where;
$\dot{h}_{net,c}$ is the net heat flux, given by convection [W/m^2]
$\dot{h}_{net,r}$ is the net heat flux, given by radiation [W/m^2]

The **net heat flux given by convection** is determined by[23]:

$$\dot{h}_{net,c} = \alpha_c \times (\Theta_g - \Theta_m) \quad [W/m^2] \tag{8.5}$$

Where;
α_c is the coefficient of heat transfer by convection [W/m^{2}K]
Θ_g is the gas temperature near the fire exposed member [^{o}C]
Θ_m is the surface temperature of the member [^{o}C]

The coefficient of heat transfer by convection, when assuming it contains the heat transfer by radiation, can be taken as 9 W/m^{2}K [23].

The **net heat flux given by radiation** is determined by [23]:

$$\dot{h}_{net,r} = \Phi \times \varepsilon_m \times \varepsilon_f \times \sigma \times [(\Theta_r + 273)^4 - (\Theta_m + 273)^4] \quad [W/m^2] \tag{8.6}$$

Where;
Φ is the configuration factor
ε_m is the surface emissivity of the member
ε_f is the emissivity of the fire
σ is the Stephan Boltzmann constant (= 5.67 x 10^{-8} W/m^{2}K)
Θ_r is the effective radiation temperature of the fire environment [^{o}C]
Θ_m is the surface temperature of the member [^{o}C]

The surface emissivity of the member can be taken as 0.8 unless other is specified [23]. The emissivity related to the concrete surface shall be taken as 0.7 [14]. The emissivity of the fire is generally taken as 1. The configuration factor should be taken as 1 unless other is specified [23].

8.4.2. Methods for design fires

The proposals from the UPTUN project is that it should be distinguished between fire scenarios where human safety are at risk and fire scenarios that concern the tunnel boundary conditions to avoid structural collapse. Where human safety is of concern, the use of heat release rate (HRR) is recommended, while for the structural resistance, the use of time-temperature curves is recommended [28]. The time-temperature curves relevant for this study is presented in the sub-chapter below.

8.5. Fire curves

Performance assessments of concrete elements with respect to fire are commonly carried out concerning fire curves [10, 15]. A lot of research has taken place to determine the types of fire that occur in tunnels and undergrounds, based on the data obtained in these researches different fire curves have been established [29]. As stated in the preliminary report to this thesis, there are mainly four different fire curves that are used in Norway [30]. The ISO 834, RWS, HC and the EUREKA fire curves. The EUREKA 60 fire curve is identical to the RABT/ZTV fire curve. The relevant fire curve is presented in figure 8-4 below, where the dark blue line represents the EUREKA 60 (RABT/ZTV train) fire curve. Bane NOR modifies the RABT/ZTV fire curve to involve three different "temperature holding" stages, holding 1200°C for 60, 90 and 120min before the cooling period, and names the fire curve EUREKA. The EUREKA fire curve is illustrated in figure 8-5 below.

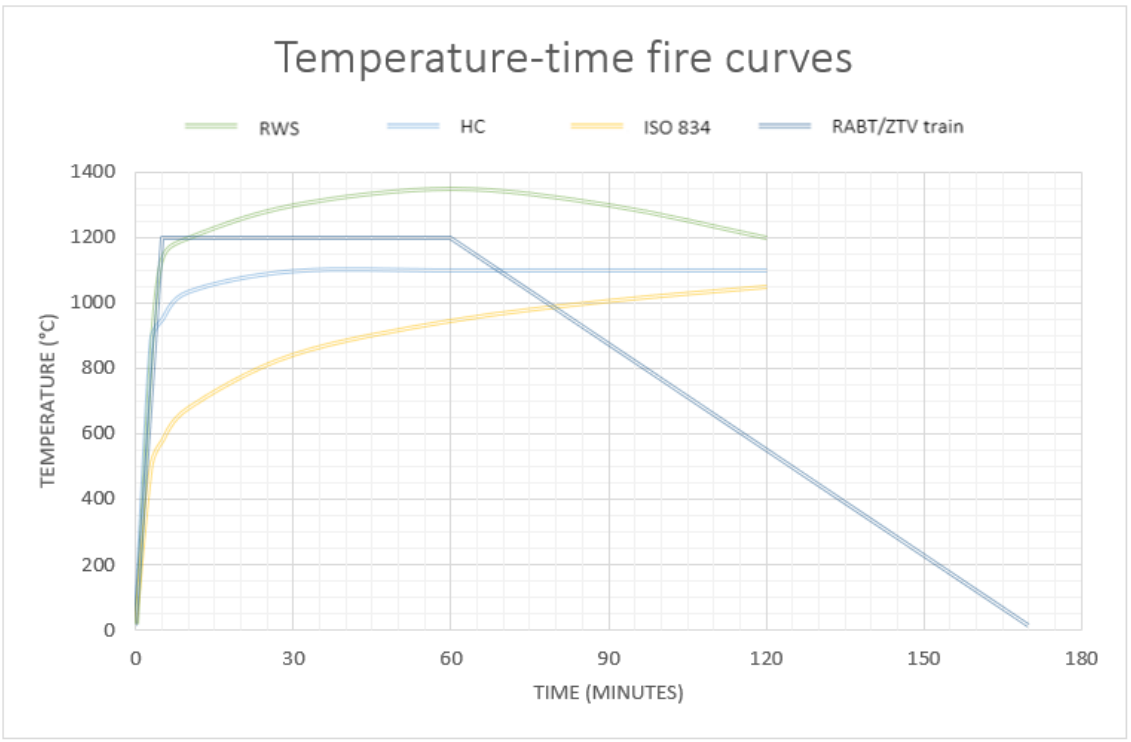

Figure 8-4 Relevant fire curves [29, 30]

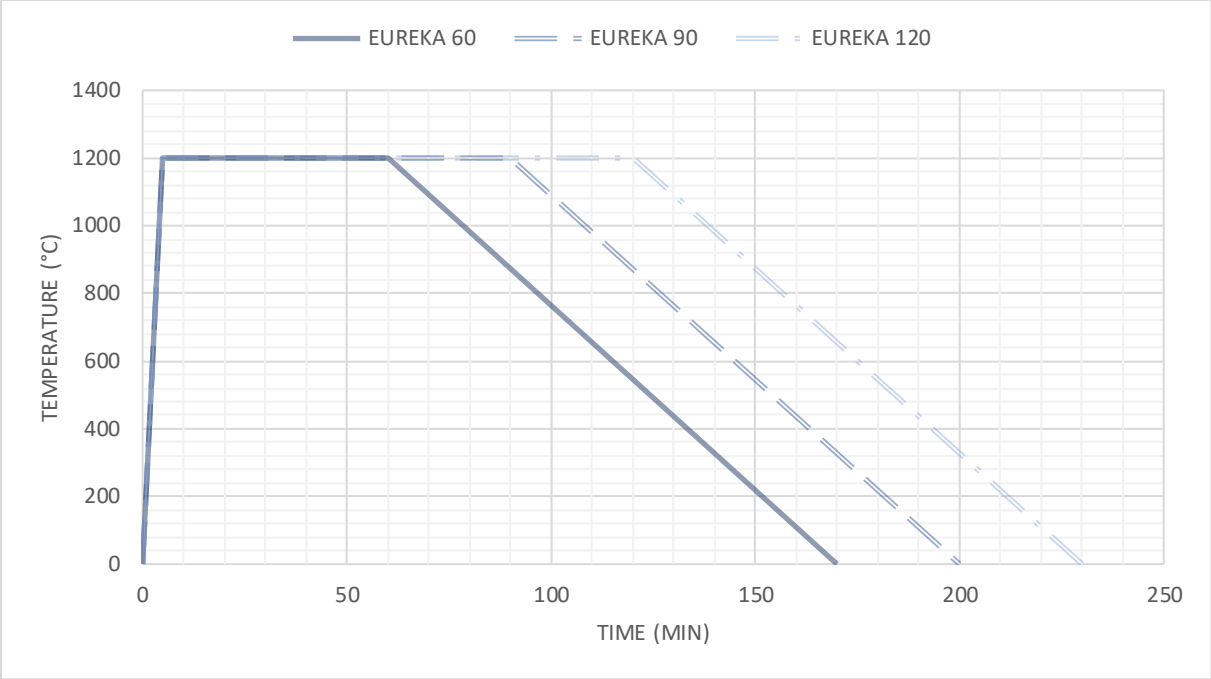

Figure 8-5 The Eureka fire curve with holding stages of 60, 90 and 120 minutes [30]

8.5.1. ISO 834

The ISO 834, standard fire curve, is a cellulosic fire curve that applies for materials found in typical buildings. This fire curve has been proved inadequate for highly combustible materials [10]. This fire curve is represented in the methods in Eurocode 2 [14].

The temperature development of the ISO 834 fire curve is described by the equation **(8.7)** below [23]:

$$T = 20 + 345 \times \log(8 \times t + 1) \quad [^{o}C] \qquad \textbf{(8.7)}$$

Where;

- T is the gas temperature in the fire compartment [^{o}C]
- t is the time [min]

8.5.2. HC

The HC, hydrocarbon fire curve, provides a rapid increase of the air temperature within a few minutes and is adequate for hazardous materials as fuels and chemicals [10]. The HC fire curve is addressed in handbook N500 [31], by the Norwegian Public Roads Administration. Where HC is defined as the dimensioning fire the fire duration is set to be 60min.

The temperature development of the ISO 834 fire curve is described by the equation **(8.8)** below [23]:

$$T = 1080 \times (1 - 0{,}325e^{-0{,}167t} - 0{,}675e^{-2{,}5t}) + 20 \quad [^{o}C] \qquad \textbf{(8.8)}$$

Where;

T is the gas temperature in the fire compartment [^{o}C]

t is the time [min]

8.5.3. RABT/ZTV

These fire curves origins from Germany and was developed through different test series such as the Eureka project [18, 29]. In this fire scenario, the temperature rises to 1200°C within 5 minutes. The RABT/ZTV fire curves separate between road and rail tunnels, where the fire curve for railway tunnels have an additional 30 min plateau before the descending phase. The descending phase is at 110 minutes for both curves [10, 18]. This fire curve is not defined by a function but by coordinates [29], as shown in table 8-2 below.

Table 8-2 The definition of the RABT/ZTV (train) fire curve [29]

RABT/ZTV [train]	
Time [minutes]	Temperature [°C]
0	15
5	1200
60	1200
170	15

The EUREKA 60 will be identical to table 8.2, while EUREKA 90 will hold 1200°C for 90 minutes and end the cooling stage after 200minutes. The EUREKA 120 will hold 1200°C for 120 minutes and end the cooling stage after 230 minutes.

8.5.4. RWS

The RWS, Rijkswaterstaat fire curve, was developed exclusively for the design of tunnels [10]. This fire curve was developed in the Netherlands, based on test results carried out by NTO in 1979. These test results were reconfirmed in the full-scale fire test in the Runehamar tunnel in Norway [29]. This fire curve is supposed to simulate tankers with a fire load of 300MW with a fire duration of 2 hours and is the severest fire curve presented [32]. This fire curve is presented in the Norwegian Public Roads Administrations handbook N400 [33]. Where the RWS fire curve is defined as the dimensioning fire the fire duration is set to 120min.

This fire scenario exceeds 1100°C within 5 minutes, and have a peak temperature at 1350°C after 1 hour [18]. This Fire curve is defined by coordinates as the RABT/ZTV fire curve [29]. This table of coordinates is presented below in table 8-3.

Table 8-3 The definition of the RWS fire curve [29]

RWS	
Time [minutes]	Temperature [°C]
0	20
3	890
5	1140
10	1200
30	1300
60	1350
90	1300
120	1200
180	1200

8.6. Modelling techniques

The finite element method has been used in this master's thesis, through the software ANSYS. The finite element method will, therefore, be briefly explained below. Important knowledge concerning the software ANSYS will also be presented here. A short introduction to the program MATLAB is also given.

8.6.1. Finite element method

The finite element method is often shortened to FEM. FEM is a mathematical technique where systems of partial differential, or integral, equations are handled. A system where the behavior cannot be predicted by closed-form equations will be suited for FEM [4].

The finite element method will produce the exact solution to an approximation of the problem that is being solved because the system can be divided into an infinite number of elements. If the system is divided into a sufficient number of elements, this approximation will be good enough to perform engineering analysis. Because the system sometimes needs to be divided into very small elements for the solution to be correct, the use of software programs is associated with FEM [4].

In finite element geometry, the nodes are used to create the elements in the model [4]. A node is a defined location in space with given DOF (degrees of freedom). The DOFs for this location, or node, represent the possible movement of this specific point due to the loading of the model. They represent which forces and moments that are transferred from one element to another. In finite element analysis, the results are usually given at the nodes [34]. A volumetric 3D model needs at least four nodes to be defined [4].

The finite element method will divide the system into small elements which have a solution, or where the solution can be approximated. This method requires that the system geometry is defined by small nodes. These nodes will each have a set of degrees of freedom, which can vary based on the inputs to the system. A set of mathematical equations will then solve the behavior of the regular shaped little elements. Each result will then be added together, and the behavior of the actual object is estimated.

As the number of elements becomes infinite, the representation of a system will approach perfection [4] [34].

A two-dimensional finite element computer program is the most accurate way to calculate the temperatures. These programs will give the temperature distribution with time over the cross-section [8]. For thermal analysis of concrete structures exposed to realistic fires, an advanced finite element calculation is recommended [8].

The accuracy of the material properties, the material model, the geometry, and loads will determine the quality of the results when using computer programs for solving problems. The computer analysis will not comment on the validity of the input parameters set in the model as long as the laws of physics are correct [4].

8.6.2. ANSYS

In any finite element analysis, there are ten basic steps to follow. The steps for the software ANSYS are presented in table 8-4 below. The ten steps are listed in order, and the module for the task in ANSYS is also given [4]:

Table 8-4 The ten basic steps of a finite element analysis [4]

10 Basic steps for a finite element analysis (ANSYS):		
Step:	**Name of the module:**	**Description:**
1	Preprocessor	Define solid model geometry
2	Preprocessor	Element types
3	Preprocessor	Material properties
4	Preprocessor	Meshing
5	Solution processor	Boundary conditions - constrains
6	Solution processor	Boundary conditions - Loads
7	Solution processor	Solution options
8	Solution processor	Solve
9	Postprocessors	Plot, view, and export
10	Postprocessors	Compare and verify

Addressing the model geometry, the different licenses of ANSYS have limitations regarding a maximum number of nodes/elements that can be applied. The student version is limited to 32 thousand elements/nodes [35].

Most of the material models in ANSYS can be temperature dependent. If there is no temperature change, or the change is of neglectable size, the material properties can be defined by one value only. In the temperature-dependent analysis, where the temperature is the degree of freedom, the analysis is classified as nonlinear because it requires an iterative solution [4].

In a transient thermal analysis, the thermal conductivity, the specific heat, and the density of the material are required [4]. A difference between a transient analysis and a static analysis is that in a transient analysis the time actually represents the time, in seconds, minutes or hours, while in a static analysis the time only represents load steps and sub-steps [36].

Usually, boundary conditions are divided into two categories. A geometric or essential boundary condition, i.e., constraints and the other natural of force boundary conditions, i.e., loads. Where the constrains is an input/output that defines the value for a given independent variable [4].

Nonlinear transient dynamic analysis where changing loads cause a time-dependent response of the system can be analyzed in ANSYS. Analyses for thermal causes can include conduction, convection, radiation, and phase changes [4].

8.6.3. MATLAB

Specifically designed for engineers and scientists, MATLAB is a programming platform. MATLAB is based on a matrix-based language and can be used for analyzing data, developing algorithms, and to create models and applications [37].

9. Research question

9.1. Issue

Through the preliminary report written in advance of this master's thesis, it emerged that there exist multiple fire curves [30]. It also emerged that the normal fire curves to be used in Norway is ISO 834, EUREKA (RABT/ZTV train), HC and RWS.

Bane NOR recommends the use of the EUREKA fire curve in their tunnel safety guidance [38] but has experienced that some consultants have ignored the recommendation. The consultants have used the ISO 834 fire curve with a longer fire duration. Bane NOR want to evaluate if this is a safe way of performing fire calculations.

9.2. Research question

To delimit the study, there is set a research question for this master's thesis.

"How do different fire loads influence the heat diffusion in load-bearing concrete tunnels?"

- What is known from the literature concerning heat diffusion in concrete tunnels exposed to fire curves?
- How should fire be modelled in the software ANSYS?
- How do the different fire curves [ISO 834, EUREKA, HC, and RWS] influence the heat diffusion in the concrete?

9.3. Limitations

This master's thesis will not evaluate how the effect of spalling will influence the temperature distribution in the concrete structure, if it occurs. The phenomena of concrete spalling will be briefly explained but will not be taken into consideration during the simulations.

The different fire curves investigated will also be limited to the ISO 834 fire curve, the HC fire curve, the RWS fire curve and the EUREKA fire curve with its three different holding stages.

10. Case

The case of this master's thesis is based on a consultant work performed for Bane NOR, on a cross-section of a load-bearing concrete tunnel. This cross-section is presented in figure 10.1 below and is obtained from Bane NOR. The recommendation from Bane NOR for performing fire calculations for this cross-section was to use the EUREKA 120 fire curve, dimensioned to withstand collapse with a fire load of 25 MW. The EUREKA 120 fire curve is illustrated in figure 8.5 in the theory chapter.

The consultants on this project chose to ignore the recommendation and performed a fire design by using the ISO 834 fire curve with a duration of 240 minutes. They stated that this, in fact, would be safer than the use of EUREKA 120 fire curve. The reason for wanting to use the ISO 834 fire curve is assumed to be that tabulated data and simplified calculation methods are available for this fire curve in the Eurocode 2. The ISO 834 fire curve are illustrated in figure 8.4 in the theory chapter.

Because the preliminary report concluded that the ISO 834, EUREKA, HC, and RWS fire curves are the most commonly used fire curves in Norway, all these fire curves will be included in the study. In this master's thesis, how the fire curves influence the heat diffusion in the concrete will be investigated. This will be performed through both a literature study and through finite element analyses performed in the software ANSYS. To perform this, how to model fire in the software has to be established. When this is settled the results from the analysis can be compared to each other and results in available research.

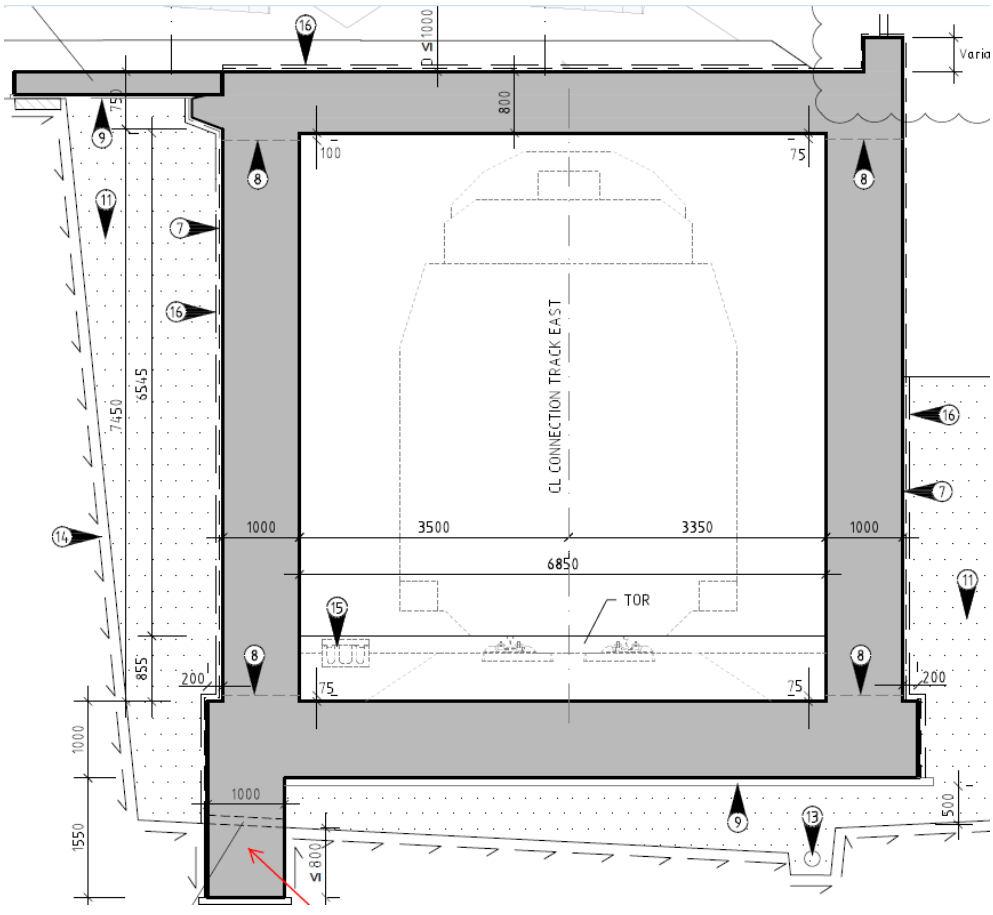

Figure 10-1 Cross-section given from Bane NOR

The goal of this study is to understand how the different fire curves will influence the heat diffusion through the concrete structure and to investigate the difference between the temperature profiles mentioned above.

To be able to answer this issue, a comprehensive literature study has been completed in addition to performing meetings with experts within the subject. People with excellent skills in the software ANSYS and people with deep understanding of fire simulations have been conferred during this master's thesis. This will be addressed in the Method chapter below.

11. Method

The method for this master's thesis is a comprehensive literature study, online tutorials, attending a course at the university, and conducting meetings. This chapter will be divided into different parts of the master's thesis, and the different methods used for each part will be described.

11.1. Literature study

To gain both broad and deep knowledge concerning the topic, a comprehensive literature study was performed. For structuring the search, presentations given by the librarian at the University of Agder was attended. The search words were checked for synonyms, and the words were combined in different compositions. The search has been performed in both English and Norwegian to maximize the outcome. This data collection began from the preliminary report written in advance of this master's thesis and derived from there. Research articles, books, and to a certain extent, encyclopedia have been examined for this search. Temperature diffusion from the Eurocode and research articles, for the relevant fire curves, were also found by this literature study.

11.2. Programs

The programs used in this master's thesis are mainly ANSYS, Excel, and MATLAB. ANSYS is used for the finite element analysis because this was the preferred software from Bane NOR. MATLAB is used to present the results from the analysis, while Excel is used to model the different fire curves.

11.3. Fire modeling

To model fire in the software turned out to be much more difficult than expected. To find relevant guidance and literature online became much more time-consuming than first presumed. This harmonized with the perception of the professors and supervisors approached in this study. Fire is a complex phenomenon and not a very common issue to investigate, specifically not with the EUREKA fire curve. To find tutorials online become difficult, and the program guides available online were not very specific. Because to simulate the fire loads in a 3D model were preferred from Bane NOR, this was the originally method. This model will be described under the result chapter.

To learn how to model fire in ANSYS, plenty of tutorials online were watched, and skype meetings with a former teacher at the university were conducted in addition to email correspondence with my supervisors. Along with this literature online and books where browsed. The book ANSYS Mechanical APDL for Finite Element Analysis [4] by Mary Kathryn Thompson and John M. Thompson was very helpful for the basic steps of the development of the initial 3D-model built during this study.

The "trial and error" methodology was attempted, where the results were analyzed on an already given assumption. The fire was first tried simulated with the ISO 834 fire curve as a fire load, where the results could be compared against the temperature profiles addressed in the Eurocode 2. This became as pointed out earlier, a very time-consuming project, where multiple approaches to the problem were simulated.

Due to the difficulty of finding guidance online for modelling fire in ANSYS, that the attendance of the course regarding fire engineering did not give answers and that the "trial and error" method became

too time-consuming, a consulting engineer that works with fire and concrete structures was contacted for help. In addition to e-mail correspondence, a meeting was conducted to get an even better insight, knowledge, and understanding.

The consulting engineer was a lifesaver that helped by establishing a model for simulating the heat diffusion of different fire curves. This model will be described under the result chapter and was modified after the different fire loads that were examined.

11.4. Selection of data

When the preferred model was selected and established, and the analyses could be modified, the selection of data had to be performed. Because the ISO 834 fire curve, the HC fire curve, the RWS fire curve and the EUREKA fire curve all are used when performing fire simulations in NORWAY this became the basis for analyses.

Since Bane NOR wants to investigate if the ISO 834 fire curve with a fire duration of 240 minutes is adequate for fire simulations within a railway tunnel fire, a comparison between the EUREKA 120 fire curve and the ISO 834 fire curve was established.

Because the goal is to investigate structural safety of concrete load-bearing tunnels during fire the critical temperature for concrete and critical temperature for the reinforcing steel was examined.

12.Results

The result chapter is divided into sub-chapters to ease the reading. First heat diffusion presented in the Eurocode and available research articles is presented. After that, different methods for how fire can be modeled in the software are addressed. Finally, the results from the modelled heat diffusion in ANSYS is presented.

12.1. Heat diffusion: Eurocode 2 and research articles

Available research articles within the topic (addressing the relevant fire curves) has been investigated, in addition to the temperature profiles presented in the Eurocode 2.

12.1.1. Heat diffusion: Eurocode 2

In the Eurocode 2 [14] a temperature distribution for slabs according to the ISO 834 fire curve is presented. The figure 12-1 below presents these temperature profiles. This figure gives the temperature distribution for the standard ISO 834 fire curve for 30-240 minutes of fire exposure. Θ is the temperature (°C), and X (mm) is the distance from the fire-exposed surface.

These temperature profiles are based on specific values. Specific heat is given with a moisture content of 1.5%, which makes the graphs conservative for moisture content greater than 1.5%. The lower limit for thermal conductivity of concrete is used, and the emissivity related to the concrete surface is set to 0.7. The convection factor is taken as 25 W/m^{2}K [14].

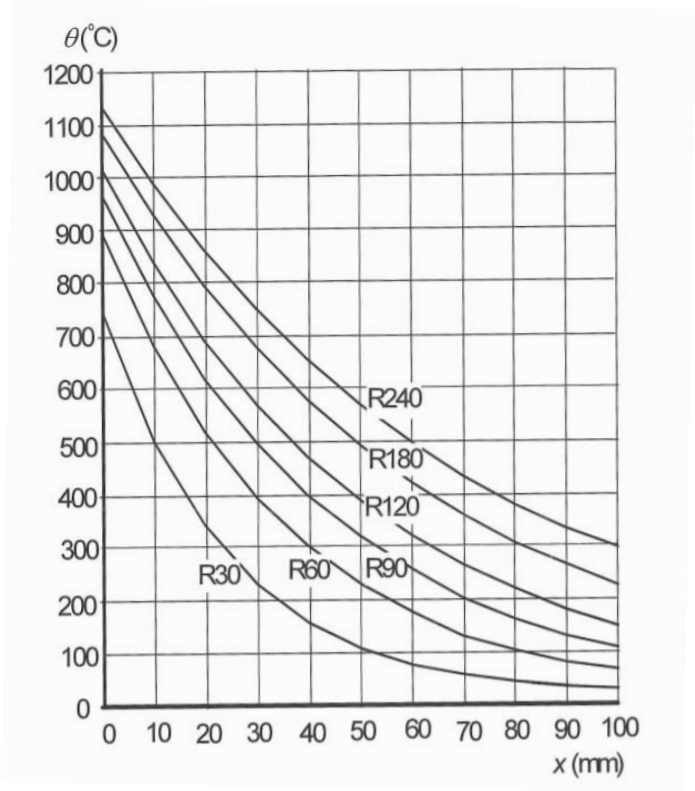

Figure 12-1 Temperature profiles for the ISO 834 standard fire curve [14]

An approximation of the heat diffusion at 60, 90, 120, and 240 minutes for figure 12-1 are presented in the table 12-1 below. The heat diffusion is given in °C, the distance from the surface is given in mm, and the values are an approximation.

Table 12-1 Heat diffusion at 60, 90,120 and 240 min for the ISO 834 fire curve, Eurocode 2

Distance from the surface [mm]	Eurocode ISO 834			
	60 min	90 min	120 min	240 min
0 mm	890°C	950°C	1010°C	1150°C
20 mm	510°C	600°C	690°C	850°C
40 mm	300°C	400°C	460°C	650°C
50 mm	220°C	325°C	400°C	575°C
60 mm	180°C	260°C	325°C	500°C
80 mm	100°C	160°C	225°C	375°C
100 mm	60°C	100°C	150°C	300°C

12.1.2. Research article by Qiao et al.

Qiao et al. [9] presented a theoretical method for investigation of the thermo-mechanical behaviors of tunnel linings subjected to the RABT/ZTV fire curve. The RABT/ZTV fire curve is presented with a holding stage of 90 minutes, which can be seen in figure 12-2 below. The analysis is based on parameters presented in table 12-2 below.

To compare their results, they compared against a finite element analysis based on the same parameters. The model for analysis consists of 23 200 four node elements, and the fire load is placed using a piecewise function directly to the inner surface. The calculation was dependent on four loading steps.

Table 12-2 Material parameters used in Qiao et al. analyzes

Parameters	Temperature dependence	Value at 20°C
Modulus of elasticity, E (GPa)		30
Poisson's ratio, μ		0.2
Thermal expansion coefficient, α (/K)		$1x10^{-5}$
Density, ρ (kg/m^3)		2400
Thermal conductivity, λ (W/mK)	1.9 – 0.00085T	1.883
Heat capacity, c (J/kgK)	836.8 + 0.4922T	913
Heat transfer coefficient, α_c (W/m^2K)	$7.05097e^{T/372.55195} + 0.84184$	8.333

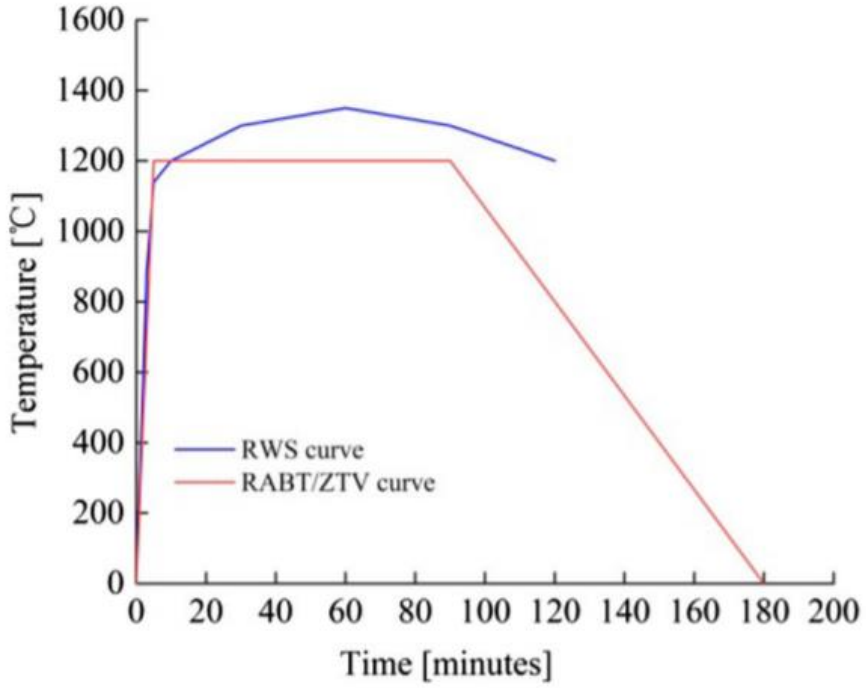

Figure 12-2 RABT/ZTV and RWS fire curves in Maraveas and Vrakas research [9]

They presented time-dependent temperature distributions at different depths, as can be seen in figure 12-3 below. To verify their results, they also performed a FEM-analysis and compared the results. The comparison can be seen in figure 12-4

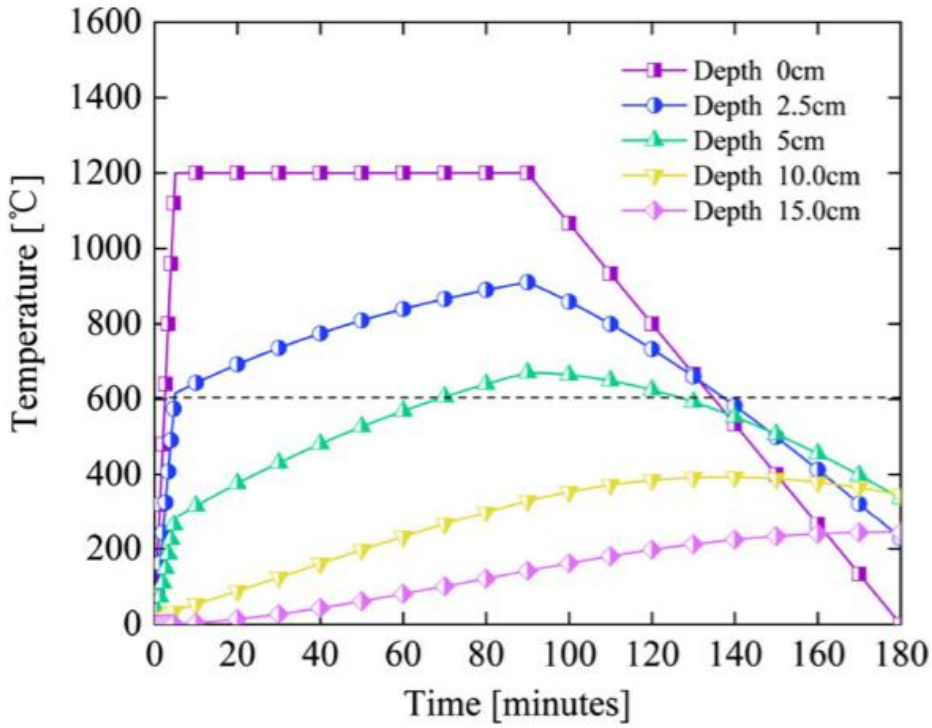

Figure 12-3 Heat diffusion, for the RABT/ZTV fire curve (theoretical method) [9]

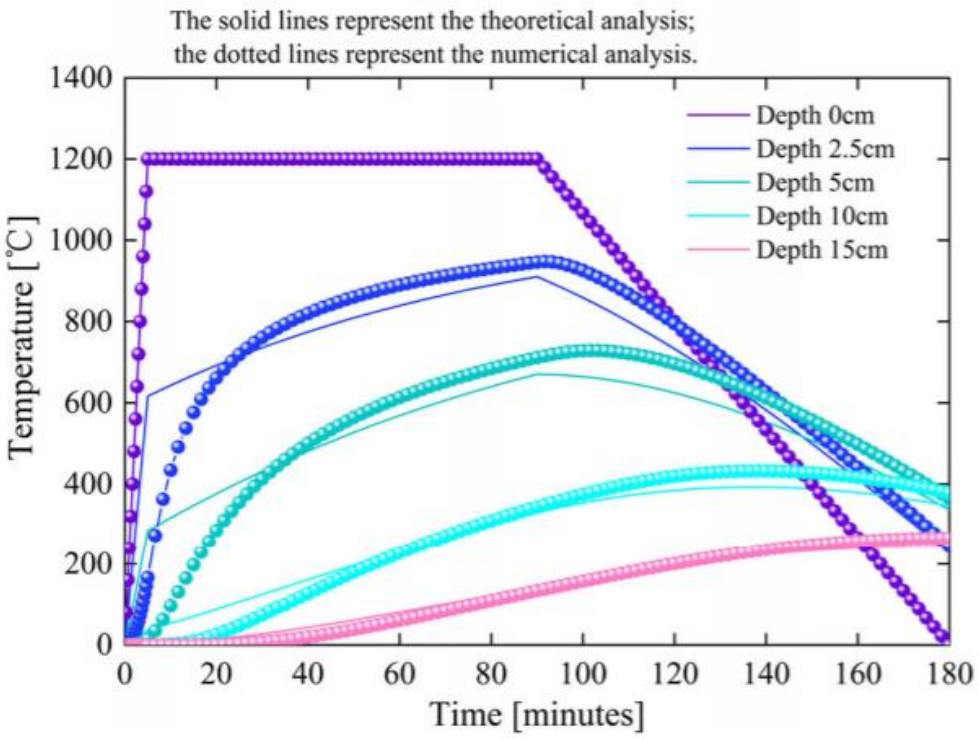

Figure 12-4 Heat diffusion for RABT/ZTV fire curve (theoretical method vs. FEM analyses) [9]

The figure 12-4 above illustrates the comparison between the theoretical method and the finite element method and shows that the results are similar. Because the results have a small deviation, the results based on the finite element analysis are used for further examination.

An approximation of the heat diffusion according to Qiao et al. at 60 min, 90 min, and 120 min for the RABT/ZTV fire curve from figure 12-4 are presented in the table 12-3 below. The heat diffusion is given in °C, and the values are an approximation

Table 12-3 Heat diffusion for the RABT/ZTV fire curve, according to Qiao et al.

Distance from surface	RABT/ZTV fire curve		
	60 min	90 min	120min
0 mm	1200°C	1200°C	800°C
50 mm	600°C	700°C	680°C
100 mm	220°C	320°C	420°C

12.1.3. Research article by Maraveas and Vrakas

Maraveas and Vrakas [10] performed a finite element analysis for multiple available fire curves. The relevant fire curves for this context is the ISO 834 fire curve, RABT/ZTV fire curve for railways, the HC fire curve, and the RWS fire curve. The RABT/ZTV train fire curve is presented with a holding stage of 60 minutes, which can be seen in figure 12-5 below.

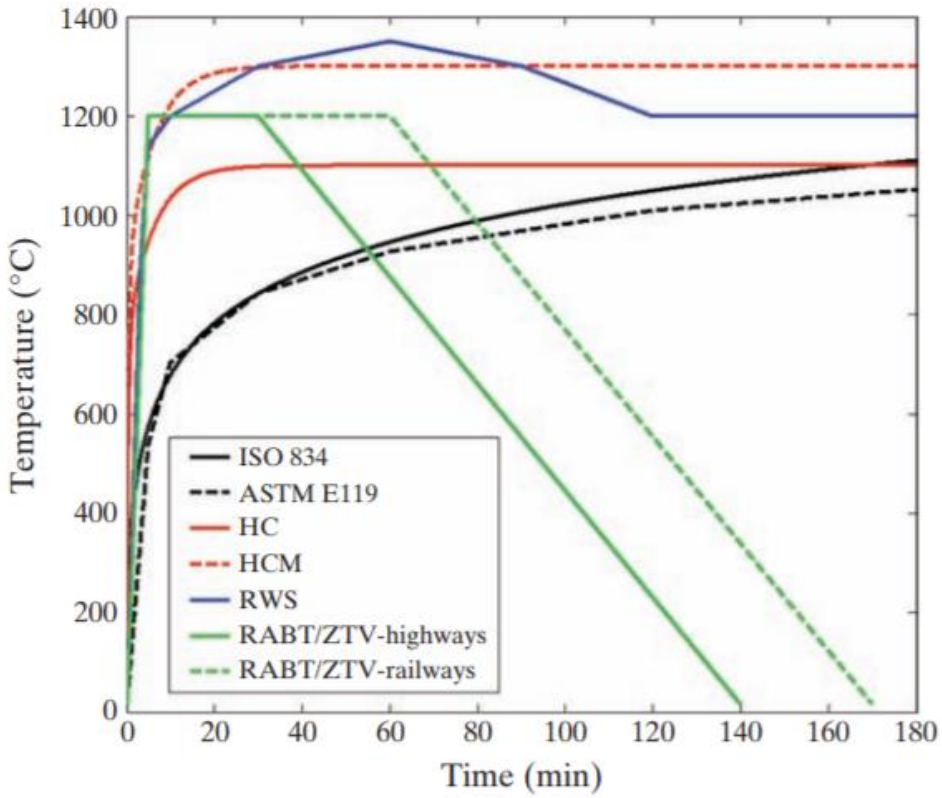

Figure 12-5 different fire curves presented in the research [10]

The analysis is performed as an uncoupled heat transfer transient finite element analysis. The model is 600 mm deep and 150 mm wide with a reinforcement of three 16 mm steel bars. The main coverage of the reinforcing steel is 45 mm.

Further, the model is built of 2D heat transfer elements. The material properties used in this article are presented in table 12-4 below. The heat is applied to the bottom surface, where no heat is transferred normal to the vertical surface.

Table 12-4 Material parameters used Maraveas and Vrakas analyzes

Parameters	Value
Convection coefficient, α_c (W/m^{2}K) [exposed side]	50
Radiation emissivity [exposed side]	0.5
Convection coefficient α_c (W/m^{2}K) [unexposed side]	9
Radiation emissivity [unexposed side]	-
Concrete density, ρ (kg/m^3)	2300
Reinforcing steel density, ρ (kg/m^3)	7850
Specific heat, c, (J/kgK)	According to Eurocode (moisture content of 3%)

The analysis shows the temperature distribution at respectively 0 mm, 20 mm, and 40 mm from the surface. This article only shows the temperature duration of 0 to 120 minutes but still gives a basis for comparison.

Figure 12-6 presents the heat diffusion at the surface, while figure 12-7 illustrates the heat diffusion at 20 mm depth. The heat diffusion of 40 mm depth is presented in figure 12.8

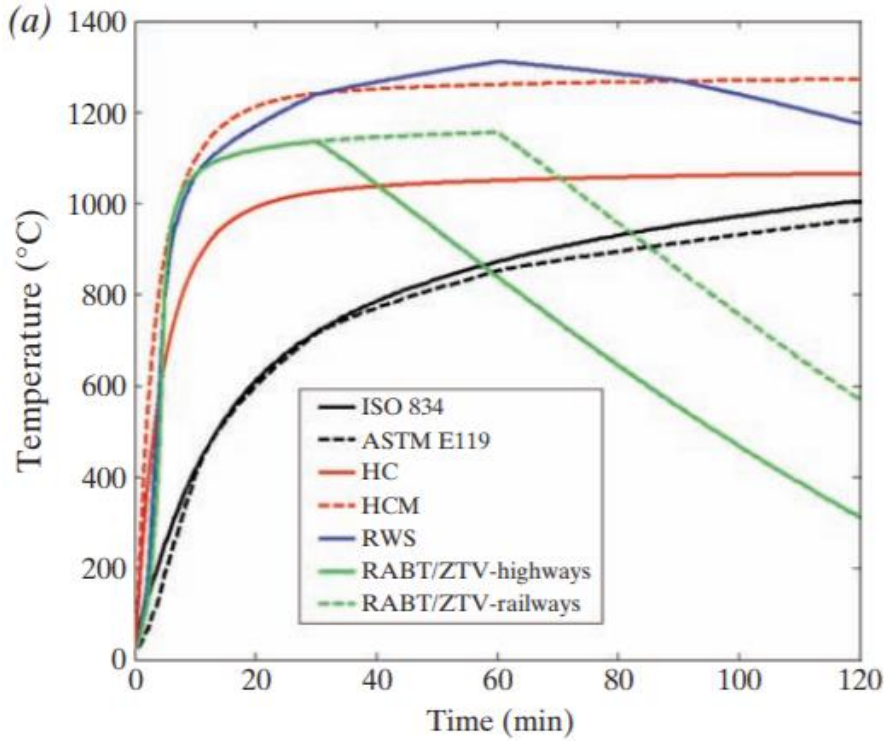

Figure 12-6 Heat diffusion for different fire curves at the surface [10]

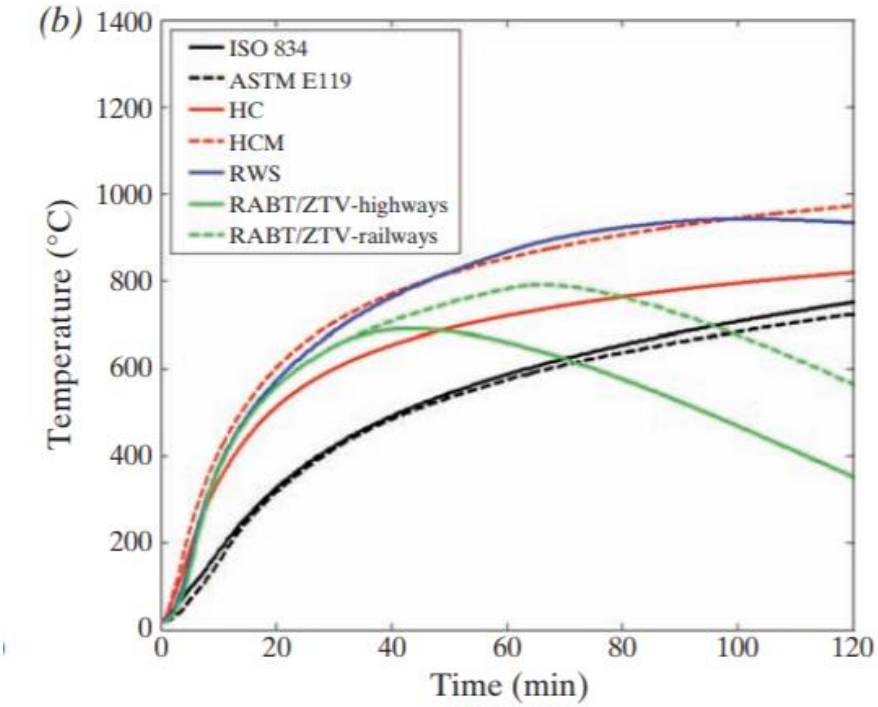

Figure 12-7 Heat diffusion for different fire curves 20mm from the surface [10]

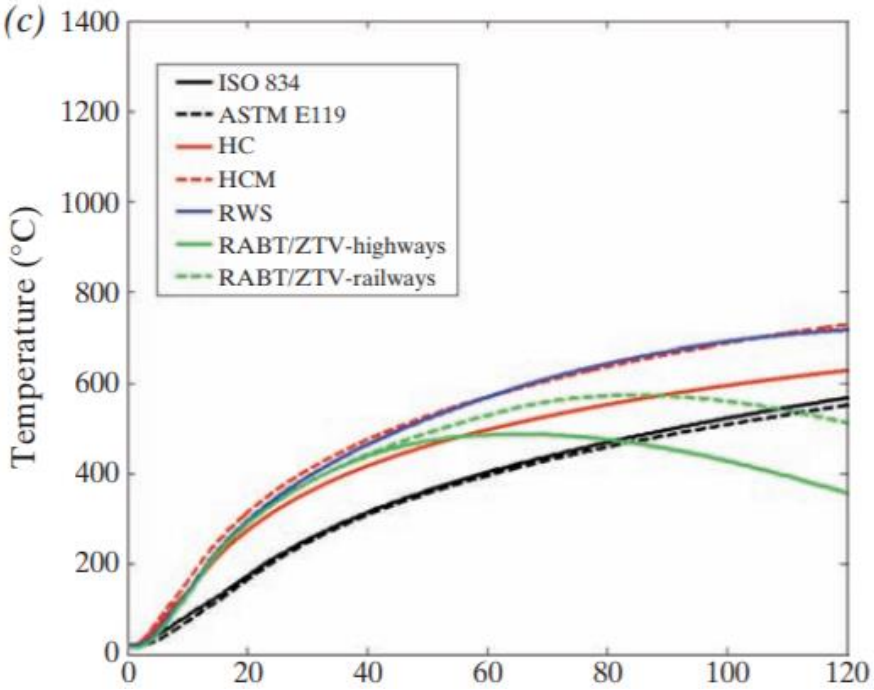

Figure 12-8 Heat diffusion for different fire curves 40 mm from the surface [10]

An approximation of the heat diffusion from figures 12-6, 12-7 and 12-8, at 60 and 120 minutes, for the ISO 834, RABT/ZTV train, RWS, and HC fire curves are presented in the table 12-5 below. The heat diffusion is given in °C, and the values are an approximation.

Table 12-5 Heat diffusion for selected fire curves according to Maraveas and Vrakas

Distance from surface	ISO 834		RABT/ZTV		RWS		HC	
	60 min	120 min	60 min	120 min	60 min	120 min	60 min	120 min
0 mm	800°C	1000°C	1100°C	600°C	1300°C	1190°C	1050°C	1100°C
20 mm	600°C	750°C	800°C	600°C	900°C	920°C	700°C	810°C
40 mm	400°C	600°C	500°C	500°C	590°C	700°C	500°C	620°C

12.1.4. Research article by Boström and Larsen

Boström and Larsen [11] presented a thermal response of tunnel concrete exposed to the RWS fire curve. This diagram was developed due to experimental testing. Conventional concrete for tunnel linings exposed to the RWS fire curve for 120 minutes, with a subsequent fast cooling phase. The results are presented in figure 12-9 below.

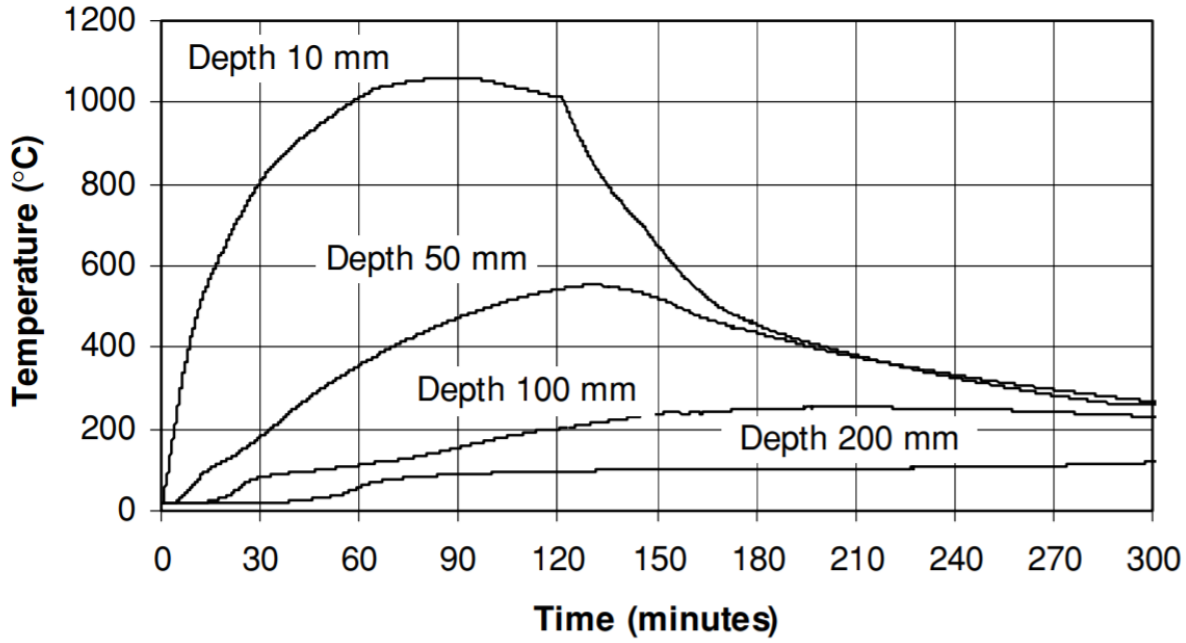

Figure 12-9 Thermal response to concrete subjected to the RWS fire curve [11]

An approximation of the heat diffusion from figure 12-9, at 60 and 120 minutes, for the RWS fire curve is presented in the table 12-6 below. The heat diffusion is given in °C, and the values are an approximation.

Table 12-6 Heat diffusion for the RWS fire curve, Boström, and Larsen.

Distance from surface	RWS	
	60 min	120 min
10 mm	1000°C	1000°C
50 mm	350°C	530°C
100 mm	110°C	200°C
200 mm	60°C	100°C

12.2. Model and material properties

Before applying the fire load a material model had to be stablished. In this sub-chapter the material properties and boundary conditions used in the model are presented.

12.2.1. Boundary conditions

The only applied load in the performed finite element analyses were the fire because of the intention of examining the heat diffusion in the concrete. The fire loads were the fire curves presented in the theory chapter, with different exposure time.

Due to the goal of this study, the solution type chosen in these analyses where a transient analysis. The time step was set to the time of interest. Throughout this study, consistency is an important factor, and all the factors and time frequencies were identical in the analysis for comparison.

12.2.2. Material properties

The material properties used in the analysis are in accordance with the Eurocode. Respectively; NS-EN 1992-1-2, NS-EN 1991-1-2 and NS-EN 1992-1-1. The convection coefficient, α_c, is only defined for the ISO 834 and the HC fire curve, respectively. The convection coefficients for the other fire curves are chosen to be the same as the HC fire curve. Why are addressed in the discussion chapter below.

The material properties used in the finite element analysis in ANSYS are presented in the table 12-7 below. Where the properties are given as a function, the properties are described further in the following sub-chapters.

Table 12-7 Material properties used in analyses in ANSYS

Parameters	Value
Specific heat, c (J/kgK)	see **(12.1) and (12.2)**
Density, ρ (kg/m^3)	see **(12.3)**
Thermal conductivity, λ (W/mK)	see **(12.4)**
Configuration factor	1
Stephan Boltzmann constant (W/m^{2}K^4)	5.67 x 10^{-8}
Emissivity related to the surface	0.7
The emissivity of the fire	1
Convection coefficient, α_c (W/m^{2}K) ISO 834	25
Convection coefficient, α_c (W/m^{2}K) EUREKA	50
Convection coefficient, α_c (W/m^{2}K) HC	50
Convection coefficient, α_c (W/m^{2}K) RWS	50

12.2.3. Specific heat

According to the NS-EN 1992-1-2 [14], the **specific heat** for concrete with **3%** moisture content in the temperature range of 20°C and 1200°C is given:

$$\begin{aligned}
&\mathrm{Cp} = 900\ \left(\frac{\mathrm{J}}{\mathrm{Kg\ K}}\right) && for\ 20^oC \le \theta \le 100^oC \\
&\mathrm{Cp,peak} = 2220\ \left(\frac{\mathrm{J}}{\mathrm{Kg\ K}}\right) && for\ 100^oC \le \theta \le 115^oC \\
&\mathrm{Cp} = 1000\ \left(\frac{\mathrm{J}}{\mathrm{Kg\ K}}\right) && 200^o\mathrm{C} \\
&\mathrm{Cp} = 1100\ \left(\frac{\mathrm{J}}{\mathrm{Kg\ K}}\right) && for\ 400^oC \le \theta \le 1200^oC
\end{aligned} \qquad (12.1)$$

It is assumed linear relationship between the given values. The graph is given in figure 12-10 below. C is the specific heat given in J/kgK, and the temperature is given in °C. The graph is modeled in ANSYS

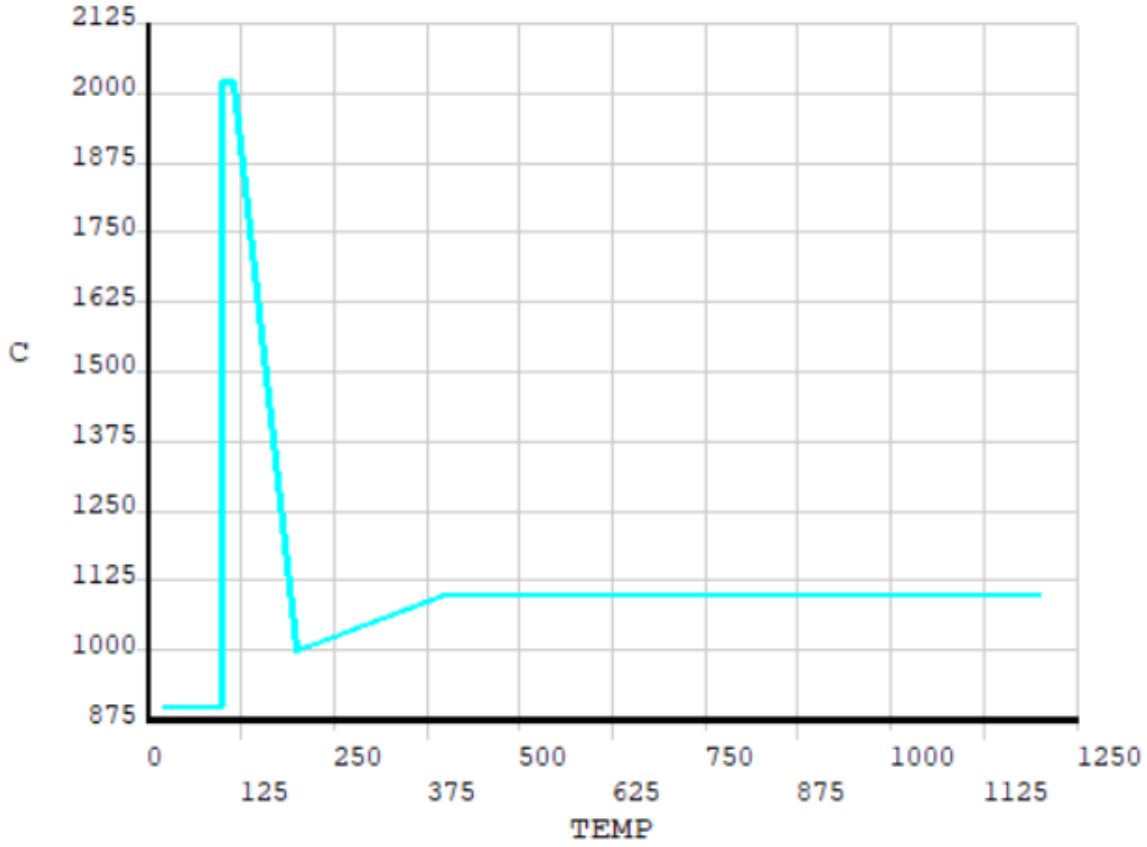

Figure 12-10 Specific heat of concrete with 3% moisture

According to the NS-EN 1992-1-2 [14], the **specific heat** for concrete with **0%** moisture content in the temperature range of 20°C and 1200°C is given:

$$\text{Cp} = 900\left(\frac{\text{J}}{\text{Kg K}}\right) \qquad for\ 20^oC \leq \theta \leq 100^oC \tag{12.2}$$

$$\text{Cp} = 900\left(\frac{\text{J}}{\text{Kg K}}\right) + (\Theta - 100) \qquad for\ 100^oC \leq \theta \leq 200^oC$$

$$\text{Cp} = 1000\left(\frac{\text{J}}{\text{Kg K}}\right) + \frac{\Theta - 200}{2} \qquad for\ 200^oC \leq \theta \leq 400^oC$$

$$\text{Cp} = 1100\left(\frac{\text{J}}{\text{Kg K}}\right) \qquad for\ 400^oC \leq \theta \leq 1200^oC$$

The graph is given in figure 12-11 below. The graph is modeled in MATLAB.

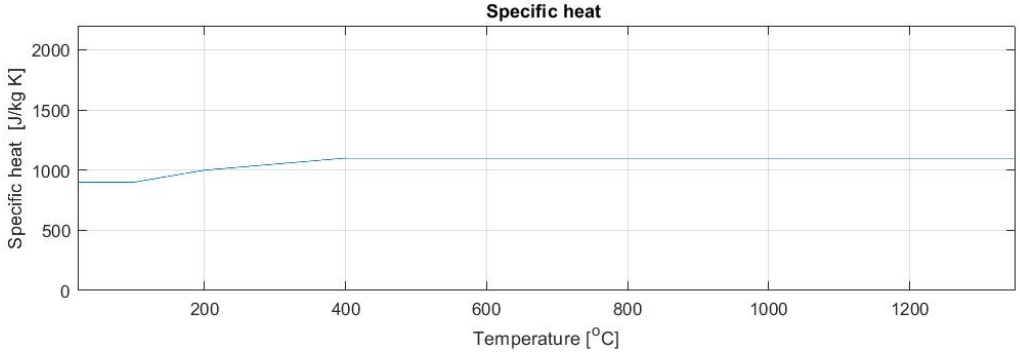

Figure 12-11 Specific heat 0% moisture content

12.2.4. Density

According to NS-EN 1992-1-2, the **density** of concrete varies with temperature because of the water loss, and can be defined as:

$$\rho(\theta) = \rho(20^oC) \qquad for\ 20^oC \leq \theta \leq 115^oC \qquad (12.3)$$
$$\rho(\theta) = \rho(20^oC)\left(1 - \frac{0.02(\theta-115)}{85}\right) \qquad for\ 115^oC \leq \theta \leq 200^oC$$
$$\rho(\theta) = \rho(20^oC)\left(0.98 - \frac{0.03(\theta-200)}{200}\right) \qquad for\ 200^oC \leq \theta \leq 400^oC$$
$$\rho(\theta) = \rho(20^oC)\left(0.95 - \frac{0.07(\theta-400)}{800}\right) \qquad for\ 400^oC \leq \theta \leq 1200^oC$$

According to NS-EN 1992-1-1 [39], the density of normal weight concrete is between 2000kg/m^3 and 2600kg/m^3. For concrete with a density of 2300kg/m^3 at 20^{o}C, the distribution will be as shown in figure 12-12 below. The graph is modeled in MATLAB

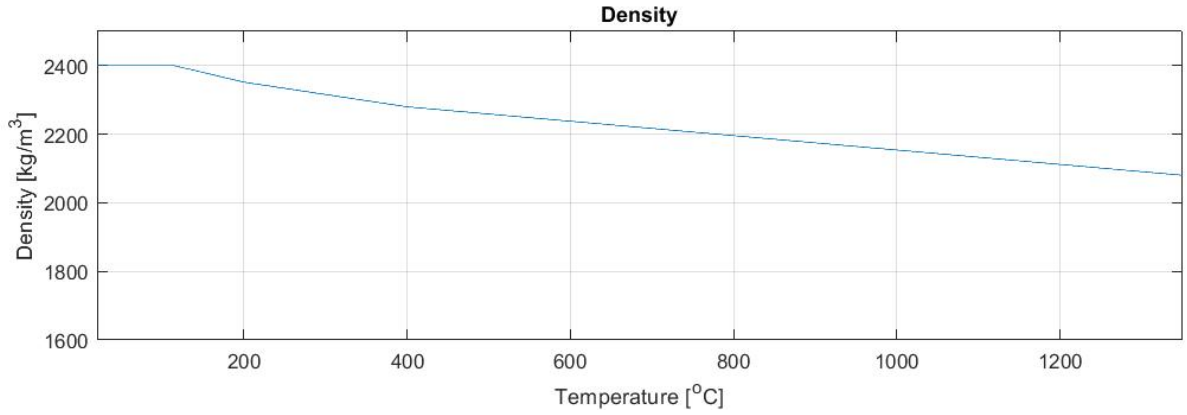

Figure 12-12 The density distribution at temperatures between 20^{o}C and 1200^{o}C

12.2.5. Thermal conductivity

According to NS-EN 1992-1-2 [14], the **thermal conductivity** of concrete is given by an upper and a lower limit. According to the Norwegian national annex, the lower limit should be used. The lower limit is given by:

$$\lambda_c = 1.36 - 0.136\left(\frac{\theta}{100}\right) + 0.0057\left(\frac{\theta}{100}\right)^2 \qquad \frac{W}{mK} \qquad (12.4)$$

The graph is modeled in MATLAB and can be seen in figure 12-13 below.

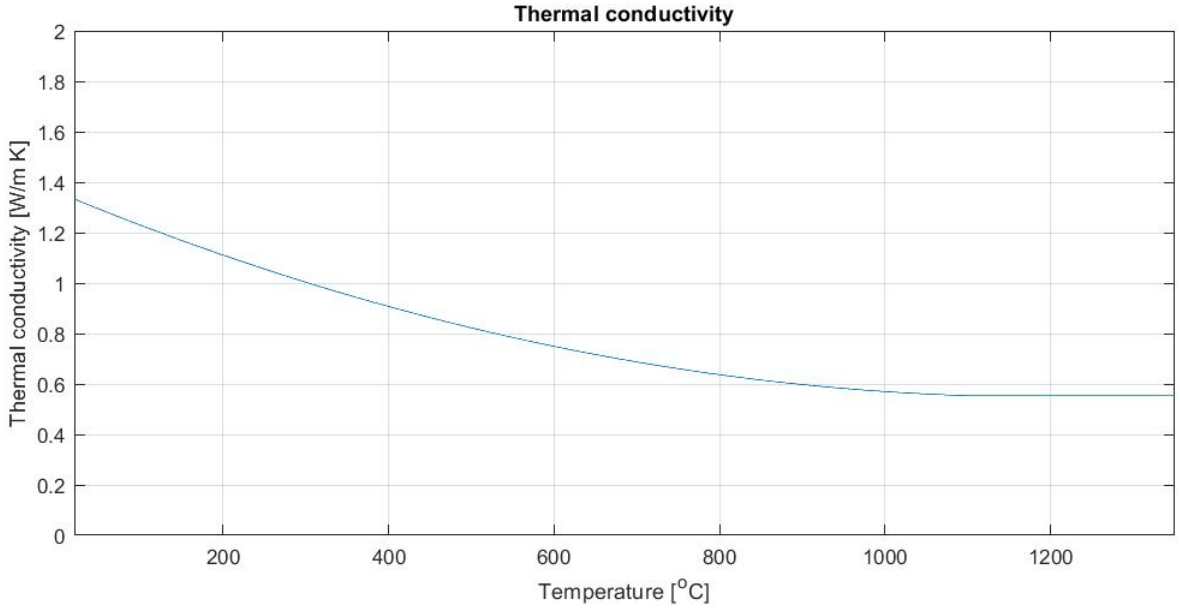

Figure 12-13 Thermal conductivity of concrete

12.3. Fire modeling in ANSYS

Two models for fire modeling in ANSYS were established. One 3D-model and one 1D-model. The models are presented below.

12.3.1. Fire modeling 3D: Conduction

The first method for finding out how to model fire in ANSYS lead in the direction of a 3D analysis with the fire curve as a thermal load on the inner surface of the tunnel. This method only considers heat transfer by conduction.

For the 3D analyses, the geometry in the ANSYS model was a simplification of the original cross-section of the tunnel. The original geometry is given in figure 10-1 in the case chapter. The geometry modeled in ANSYS is illustrated in figure 12-14 below. The dimensions are given in table 12-8 below.

Table 12-8 Geometry of the cross-section modeled in ANSYS for 3D simulations

The geometry of the cross-section	
B (m)	8.85
H (m)	9.2
W (m)	1
t_b (m)	1
t_w (m)	1
t_t (m)	0.8

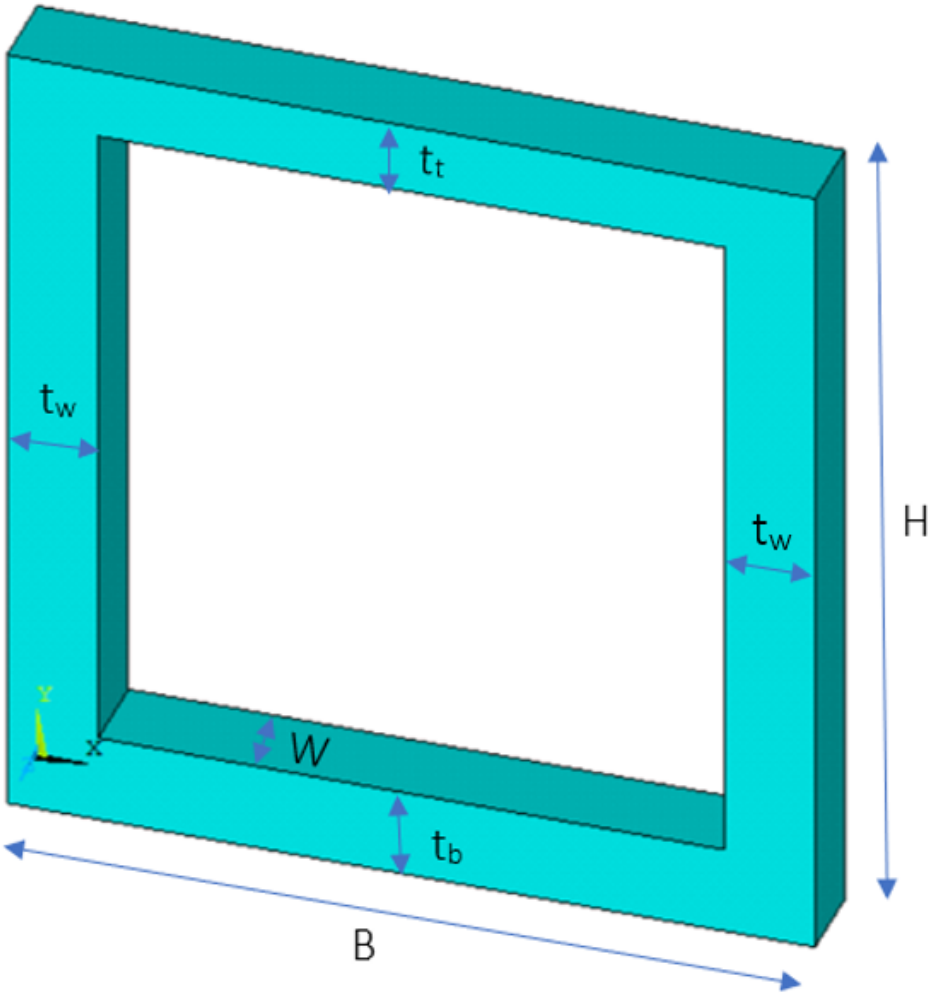

Figure 12-14 The modified cross-section modeled in ANSYS for 3D simulations

The geometry was defined by the "Top Down" method described in [4]. Where the model was created by defining two blocks and subtracting the smaller block by using the boolean operator.

The element type used in the 3D-analyses were the SOLID278. This element has a 3D thermal conductivity capability and has 8 nodes with a temperature degree of freedom at each node. This element can be used for a 3D transient thermal analysis. This element and be used both for applying convection and heat flux as the surface load at the element faces, but not both at the same time. In addition to one of the two mentioned above, radiation can also be applied similarly [40].

No real constants are required for the element SOLID278, but the material properties that have to be defined are the materials thermal conductivity, the density of the material, and its specific heat. The thermal conductivity is defined as a 9x9 matrix, with 9 possible constants. Because the material is isotropic, the thermal conductivity only has to be defined in X-direction [41]. The specific heat for this analysis was defined by an assumption of moisture content of 3%. The element properties of the SOLID278 are presented in table 12-9 below.

Table 12-9 Properties of the SOLID278 element

Name	SOLID278 [40]
Type	3D element
Number of nodes	8
Degree of freedom	Temperature
Ability	Solid heat conduction
Real Constants	
Material properties	Thermal conductivity, density, and specific heat

Because the meshing of the element is very crucial for the results, a finer mesh was desirable. The student version of ANSYS has a limitation of number of nodes and elements [35], which indicated that the geometry had to be re-evaluated. As the fire is presumed to be highest at the ceiling [13], a new model consisting only the ceiling was developed. Here a finer mesh was obtained, with an element edge length of 0.15m. The figure 12-15 below shows the meshing of the ceiling.

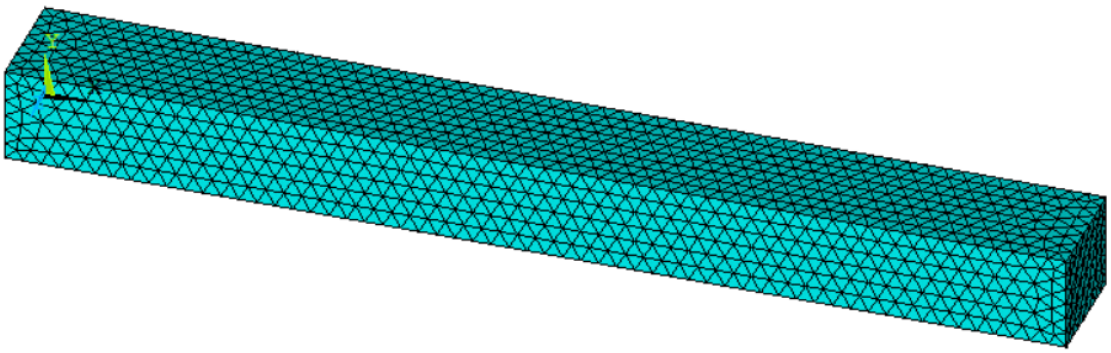

Figure 12-15 Final mesh for the 3D-model

The results were plotted as a nodal solution on the temperature degree of freedom and showed the temperature diffusion in the section. The results were also shown as a graph with a plotted path for the middle of the fire exposed top slab. The results for this model is presented in chapter 12.4

12.3.2. Fire modeling 1D: Conduction, convection, and radiation

By adding conduction, convection, and radiation elements, the 1D-model considers all three forms of heat transfer. This model is built upon 200 LINK33 1D conduction elements over the thickness, one LINK 34 convection element on each side and one LINK 31 radiation element on the fireside. The elements have a depth of 400mm.

The nodes were placed with 2mm distance, where the first node is placed as a space node 2mm from the inner surface of the tunnel. The fire was then simulated as a gas-temperature load on the space node. The calculations are performed as a transient temperature analysis over 360 minutes with a time step of 20 seconds.

In this analysis, the element types LINK31, LINK 33 and LINK34 were all applied in the model. Element type link 31 is a uniaxial element that models the radiation heat flow between two points in space. This element is defined by two nodes, with a temperature degree of freedom at each node [42]. Element type LINK33 is a uniaxial element with the ability to conduct heat between its nodes. This element is defined by two nodes, with a temperature degree of freedom at each node [43]. Element type LINK34 is a uniaxial element with the ability to convect heat between its nodes. This element is defined by two nodes, with a temperature degree of freedom at each node [44].

Real constants required for the element LINK31 is the radiating surface area, the geometric form factor, the emissivity, and the Stefan-Boltzmann constant [42]. For the element LINK33, the cross-sectional area is a required constant. Material properties that must be defined are the density, the thermal conductivity, the specific heat, and the enthalpy. The thermal conductivity is in the element longitudinal direction [43]. The real constants required for the element LINK34 is the convection surface area, the empirical coefficient, and the input constant. Material properties that have to be defined are the convection or film coefficient [44]. The properties that must be defined for the elements used in this model are defined in table 12-10 below. For these analyses, the specific heat was defined by assuming a moisture content of 0%. This will make the temperature graphs conservative for moisture contents greater than 0% [14].

Table 12-10 Properties of the used elements in the 1D model

Name	LINK31 [42]	LINK33 [43]	LINK34 [44]
Type	Uniaxial element	Uniaxial element	Uniaxial element
Number of nodes	2	2	2
Degree of freedom	Temperature	Temperature	Temperature
Ability	Radiation heat flow between two points in space	Conduct heat between its nodes	Convect heat between its nodes
Real Constants	Radiating surface area, geometric form factor, emissivity, and the Stefan-Boltzmann constant	Cross-sectional area	Convection surface area, empirical coefficient and the input constant
Material properties		Density, thermal conductivity, specific heat, and the enthalpy	convection or film coefficient

12.4. Heat diffusion 3D model – ANSYS

Two different loading approaches with the 3D model is presented in the sub-chapter below. The results from these analyses are discussed in chapter 13.2.

12.4.1. Fire curve as surface load

The fire load was placed by the function for the ISO 834 **(equation 8.7)** fire curve as a temperature load on the surface area of the tunnel ceiling. The results for a fire exposure of 240 minutes are shown in figures 12-16 and 12-17 below. TEMP is the temperature in °C and DIST is the distance from the surface in meters.

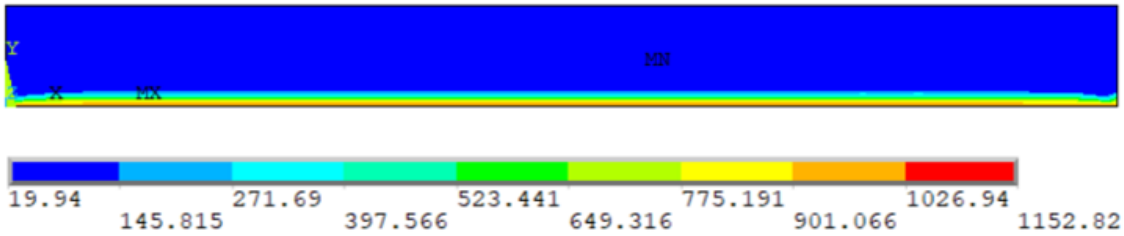

Figure 12-16 Heat diffusion after 240 minutes exposed to the ISO 834 fire curve, 3D model

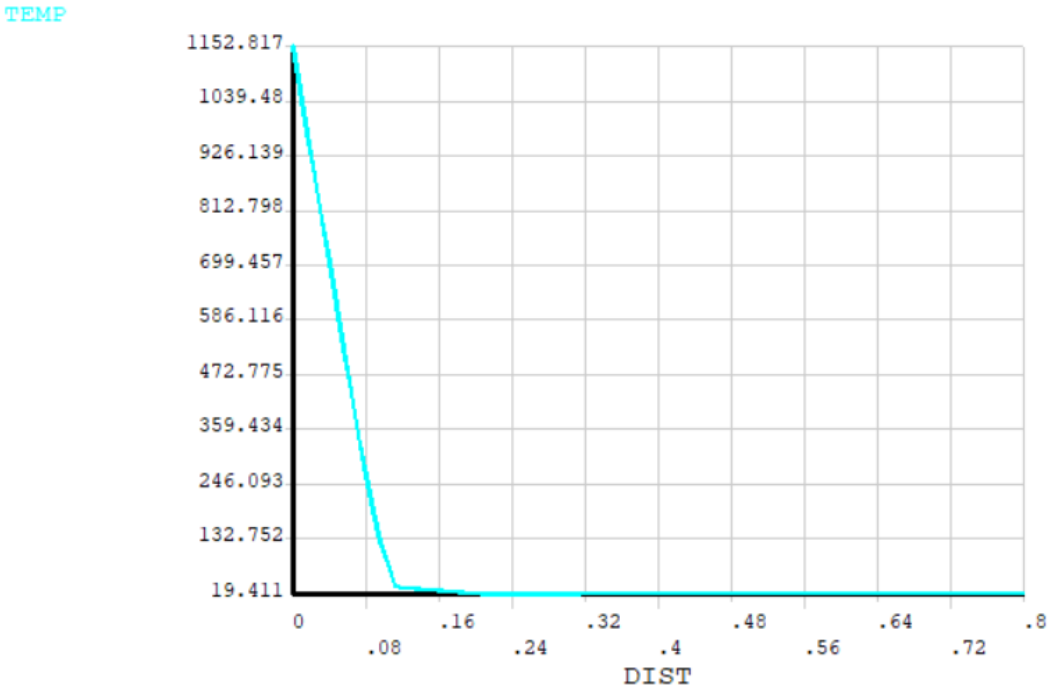

Figure 12-17 Heat diffusion after 240 minutes exposed to the ISO 834 fire curve, 3D model

The results of this analysis are presented in the table 12-11 below, for 60, 120, and 240 minutes of time duration.

Table 12-11 Heat diffusion for the ISO 834 fire curve for the 3D model

Distance from surface	ISO 834, ANSYS		
	60 min	120 min	240 min
0 mm	945.34°C	1049.04°C	1152.82°C
20 mm	760.245°C	843.175°C	926.139°C
40 mm	575.149°C	637.307°C	699.457°C
60 mm	390.053°C	431.439°C	472.775°C
80 mm	204.957°C	225.571°C	246.093°C

12.4.2. Constant value as fire load

The fire load was placed as a constant temperature on the inner surface of the tunnel ceiling. The constant temperature was chosen to be the maximum temperature of the ISO 834 fire curve **(equation 8.7)** at 60, 120, and 240 minutes of fire exposure. The figures 12-18 and 12-19 below presents the results of the analysis for 240 minutes. TEMP is the temperature in °C and DIST is the distance from the surface in meters.

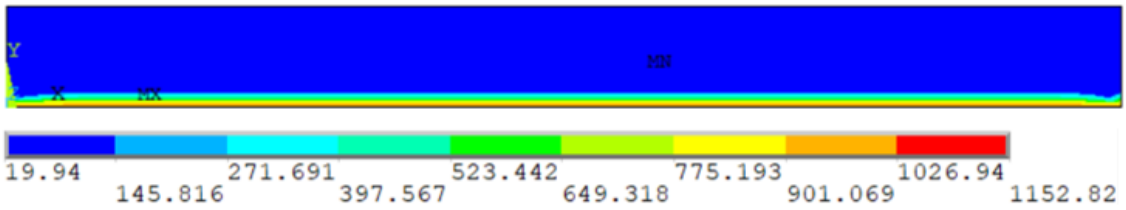

Figure 12-18 Heat diffusion for a constant value of 1152.82°C for 240 minutes, 3D model

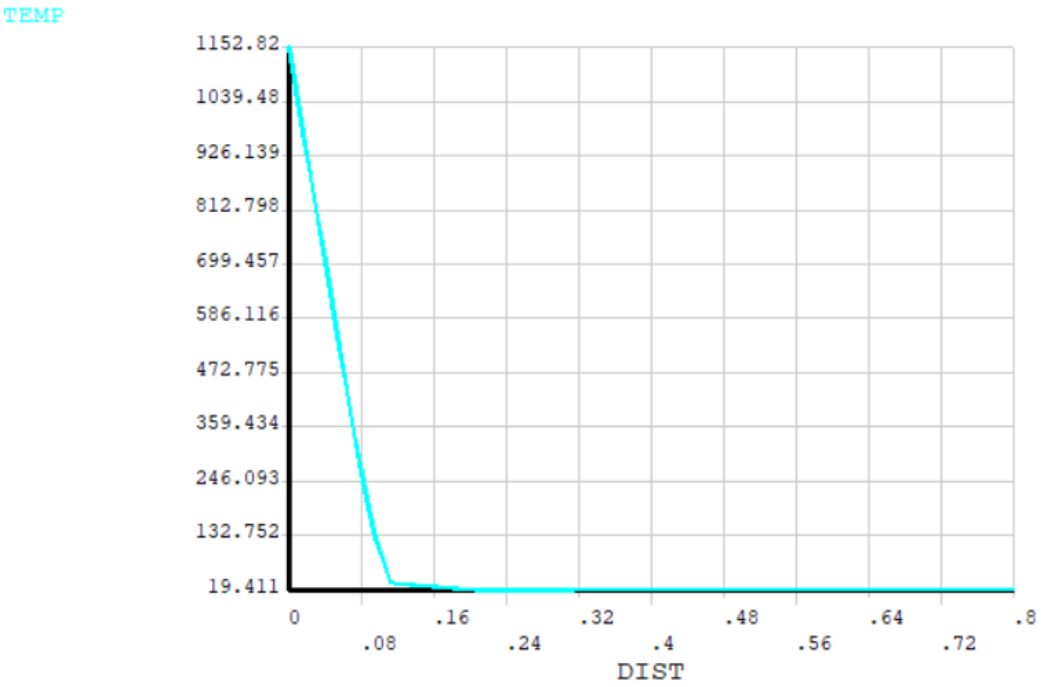

Figure 12-19 Heat diffusion for a constant value of 1152.82°C for 240 minutes, 3D model

The results from this analysis are presented in the table 12-12 below for the time duration of 60, 120, and 240 minutes.

Table 12-12 Heat diffusion for the 3D model with constant values

Distance from surface	ISO 834, ANSYS		
	60 min	120 min	240 min
0 mm	945.34°C	1049.04°C	1152.82°C
20 mm	760.245°C	843.175°C	926.139°C
40 mm	575.149°C	637.307°C	699.457°C
60 mm	390.053°C	431.439°C	472.775°C
80 mm	204.957°C	225.571°C	246.093°C

12.5. Heat diffusion 1D model – ANSYS

For the 1D model all the fire curves were used as a loading condition in the analyses. Analyses performed with all four fire curves as a fire load will be presented in this result chapter. The EUREKA fire curve will be presented for a holding stage of 60 min, 90 min and 120 minutes. The fire curve was placed as a thermal load on the space node as a gas-temperature load.

12.5.1. ISO 834

The loading for this scenario was the ISO 834 fire curve, described in the theory chapter, equation **(8.7)**. The temperature diffusion in the concrete is presented in figure 12-20 below. The temperature profiles presented are for 60 min, 90 min, 120 min, and 240 min.

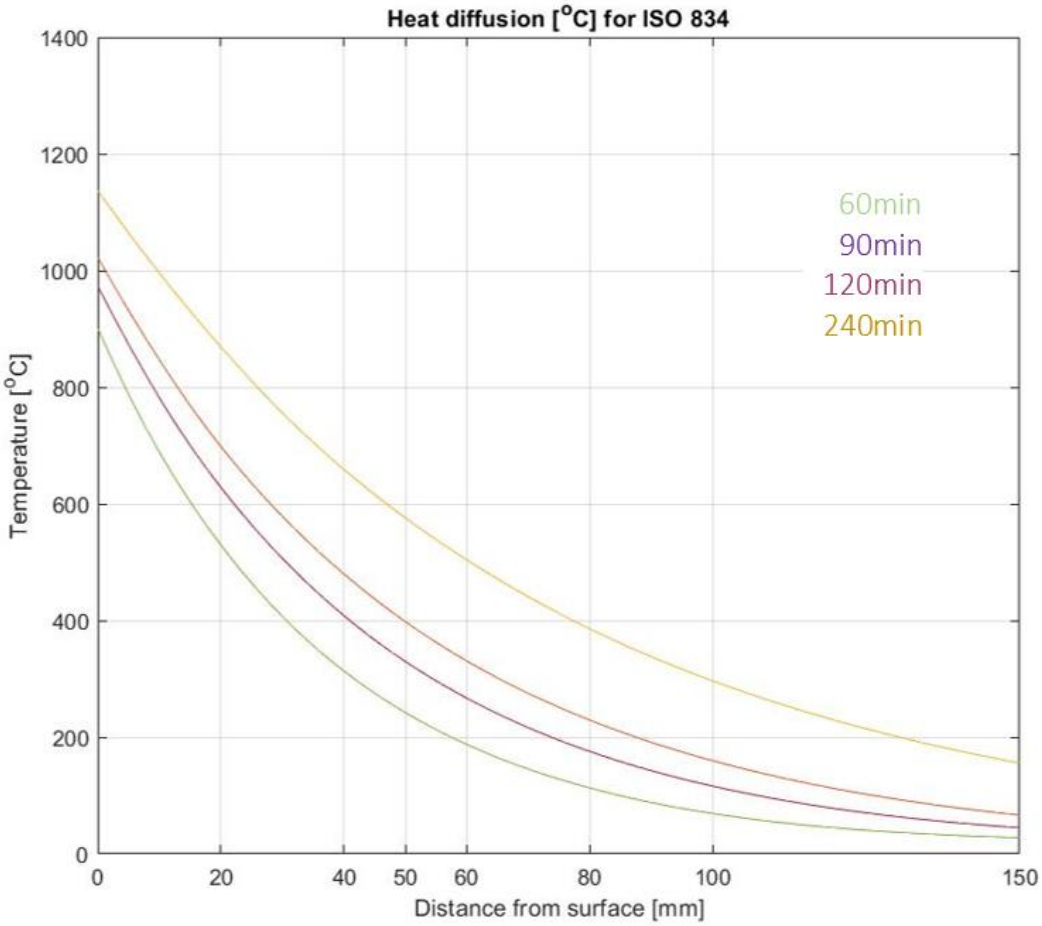

Figure 12-20 Heat diffusion for the ISO 834 fire curve, 1D model

The Heat diffusion at selected distances from the surface is presented in the table 12-13 below. The values are an approximation.

Table 12-13 Heat diffusion for selected depths for the ISO 834 fire curve, 1D model

Distance from surface	ISO 834, ANSYS 1D			
	60 min	90 min	120 min	240 min
0 mm	900°C	975°C	1020°C	1140°C
20 mm	530°C	630°C	700°C	870°C
40 mm	315°C	410°C	480°C	660°C
50 mm	240°C	330°C	400°C	575°C
60 mm	190°C	270°C	330°C	505°C
80 mm	115°C	175°C	230°C	385°C
100mm	70°C	115°C	160°C	295°C

12.5.2. EUREKA 60

The loading for this scenario was the EUREKA 60 fire curve, described in the theory chapter, figure 8-5. The heat diffusion is presented in figure 12-21 below. The temperature profiles presented are 60 min, 90 min, 120 min, and 240 min.

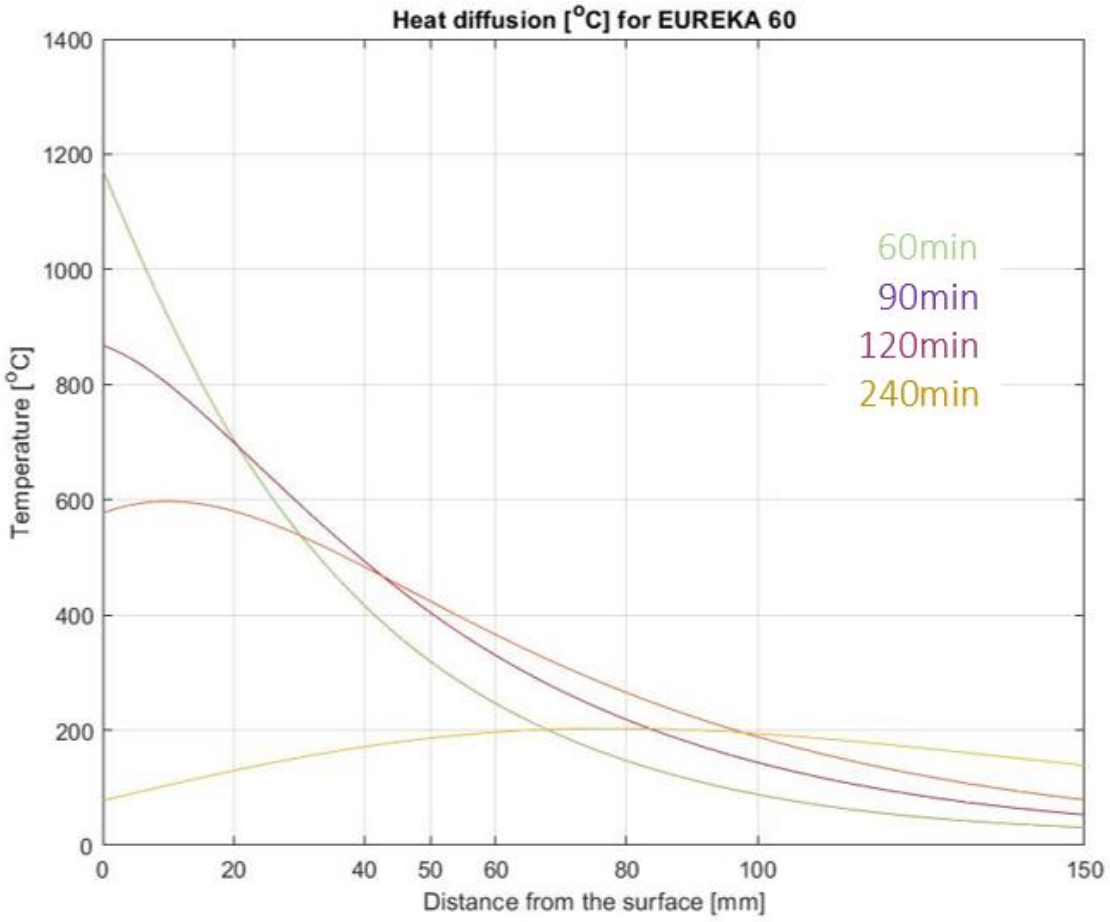

Figure 12-21 Heat diffusion for the EUREKA 60 fire curve, 1D model

The Heat diffusion at selected distances from the surface is presented in the table 12-14 below. The values are an approximation.

Table 12-14 Heat diffusion for selected depths for the EUREKA 60 fire curve, 1D model

Distance from surface	EUREKA 60, ANSYS 1D			
	60 min	90 min	120 min	240 min
0 mm	1173°C	870°C	575°C	80°C
20 mm	705°C	700°C	580°C	130°C
40 mm	415°C	495°C	485°C	170°C
50 mm	320°C	405°C	425°C	185°C
60 mm	245°C	330°C	365°C	195°C
80 mm	145°C	220°C	265°C	205°C
100mm	90°C	145°C	190°C	195°C

12.5.3. EUREKA 90

The loading for this scenario was the EUREKA 90 fire curve, described in the theory chapter, figure 8-5. The heat diffusion is presented in figure 12-22 below. The temperature profiles presented are 60 min, 90 min, 120 min, and 240 min.

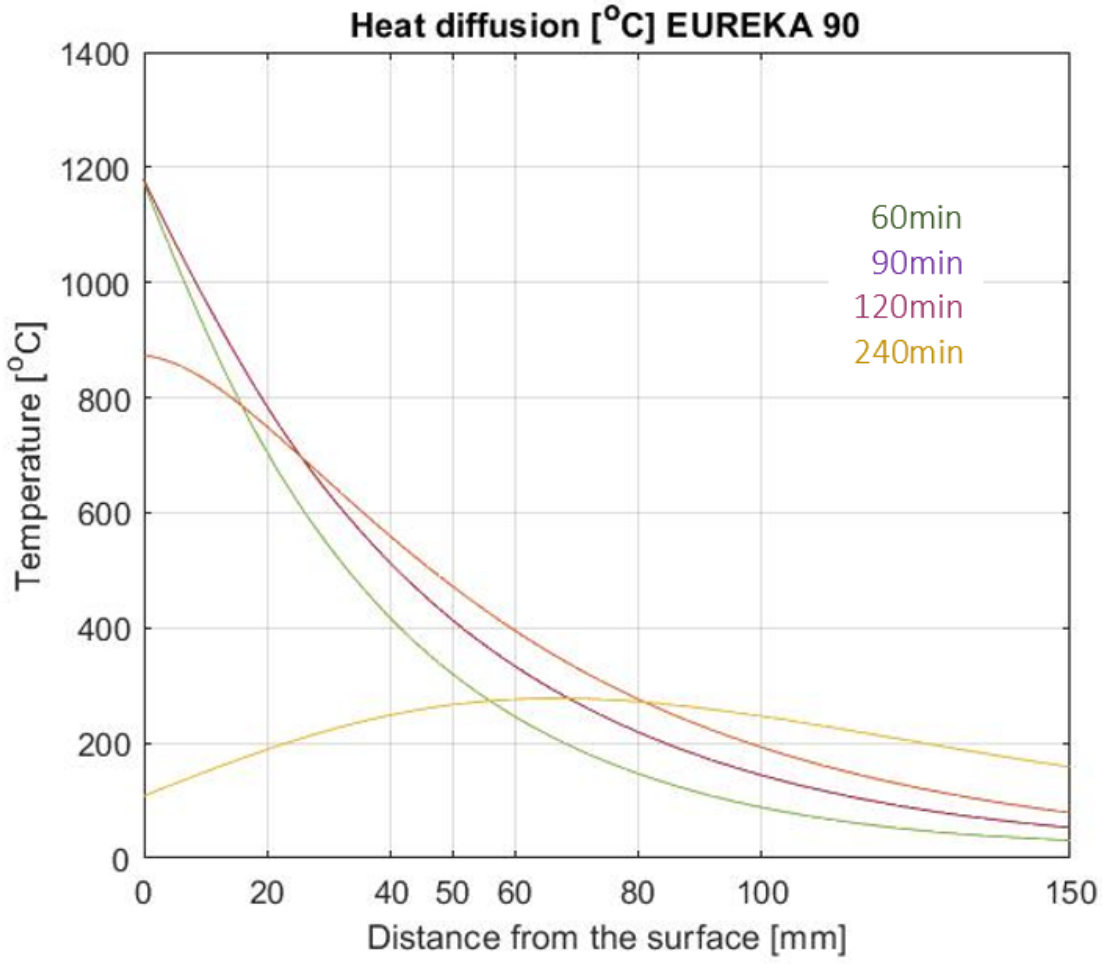

Figure 12-22 Heat diffusion for the EUREKA 90 fire curve, 1D model

The Heat diffusion at selected distances from the surface is presented in the table 12-15 below. The values are an approximation.

Table 12-15 Heat diffusion at selected depths for EUREKA 90, 1D model

Distance from surface	EUREKA 90, ANSYS 1D			
	60 min	90 min	120 min	240 min
0 mm	1173°C	1178°C	875°C	110°C
20 mm	705°C	785°C	750°C	190°C
40 mm	415°C	510°C	560°C	250°C
50 mm	320°C	415°C	475°C	265°C
60 mm	245°C	335°C	395°C	275°C
80 mm	145°C	220°C	275°C	270°C
100mm	90°C	145°C	195°C	245°C

12.5.4. EUREKA 120

The loading for this scenario was the EUREKA 120 fire curve, described in the theory chapter, figure 8-5. The heat diffusion is presented in figure 12-23 below. The temperature profiles presented are 60 min, 90 min, 120 min, and 240 min.

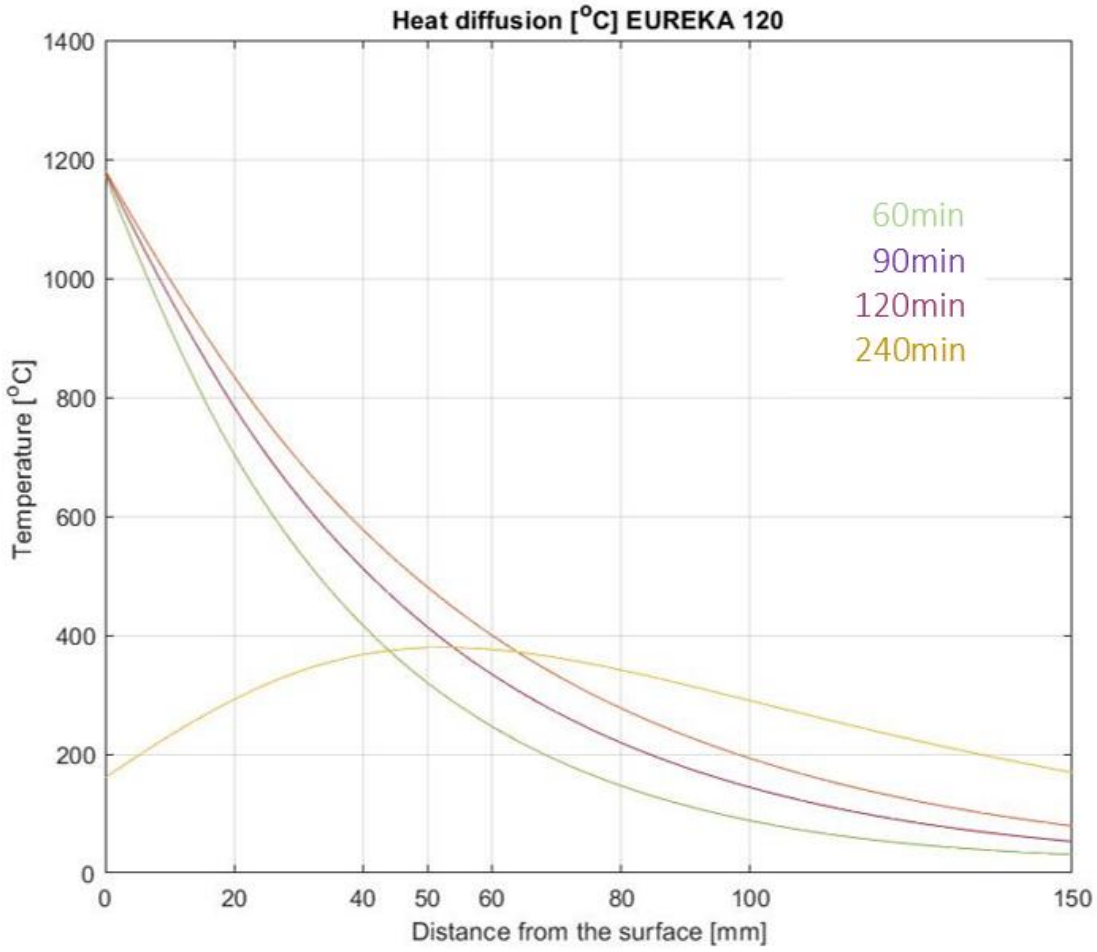

Figure 12-23 Heat diffusion for EUREKA 120, 1D model

The Heat diffusion at selected distances from the surface is presented in the table 12-16 below. The values are an approximation.

Table 12-16 Heat diffusion for EUREKA 120min, 1D model

Distance from surface	EUREKA 120, ANSYS 1D			
	60 min	90 min	120 min	240 min
0 mm	1173°C	1178°C	1181°C	160°C
20 mm	705°C	785°C	835°C	290°C
40 mm	415°C	510°C	575°C	365°C
50 mm	320°C	415°C	480°C	380°C
60 mm	245°C	335°C	400°C	375°C
80 mm	145°C	220°C	280°C	340°C
100mm	90°C	145°C	195°C	290°C

12.5.5. RWS

The loading for this scenario was the RWS fire curve, described in the theory chapter, table 8-3. The heat diffusion is presented in figure 12-24 below. The temperature profiles presented are 60 min, 90 min, 120 min, and 240 min.

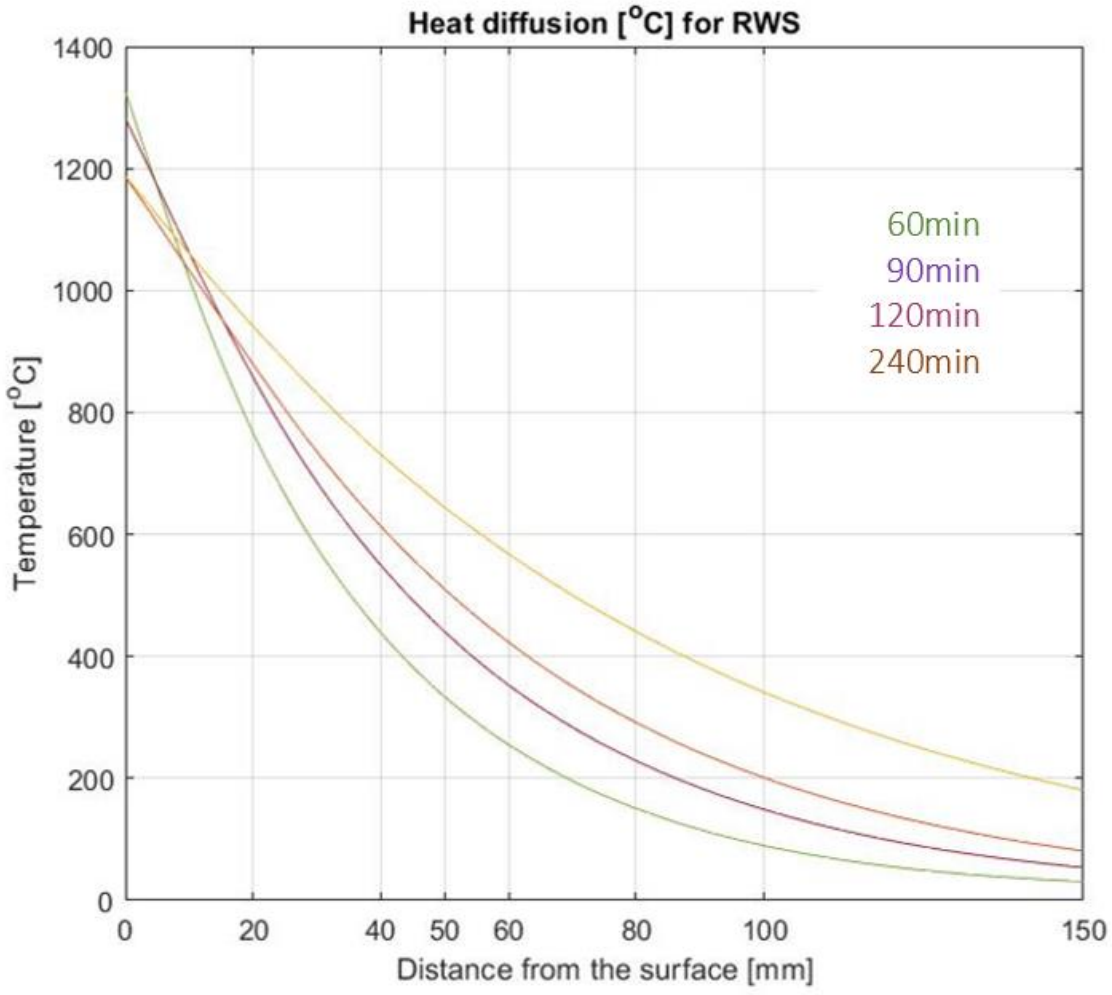

Figure 12-24 Heat diffusion for the RWS fire curve, 1D model

The Heat diffusion at selected distances from the surface is presented in the table 12-17 below. The values are an approximation.

Table 12-17 Heat diffusion for selected depths for the RWS fire curve, 1D model

Distance from surface	RWS, ANSYS 1D			
	60 min	90 min	120 min	240 min
0 mm	1326°C	1282°C	1187°C	1190°C
20 mm	765°C	860°C	880°C	940°C
40 mm	440°C	550°C	615°C	730°C
50 mm	335°C	440°C	510°C	645°C
60 mm	255°C	355°C	425°C	570°C
80 mm	150°C	230°C	290°C	440°C
100mm	90°C	150°C	200°C	340°C

12.5.6. HC

The loading for this scenario was the HC fire curve, described in the theory chapter, equation **(8.8)**. The heat diffusion is presented in figure 12-25 below. The temperature profiles presented are 60 min, 90 min, 120 min, and 240 min.

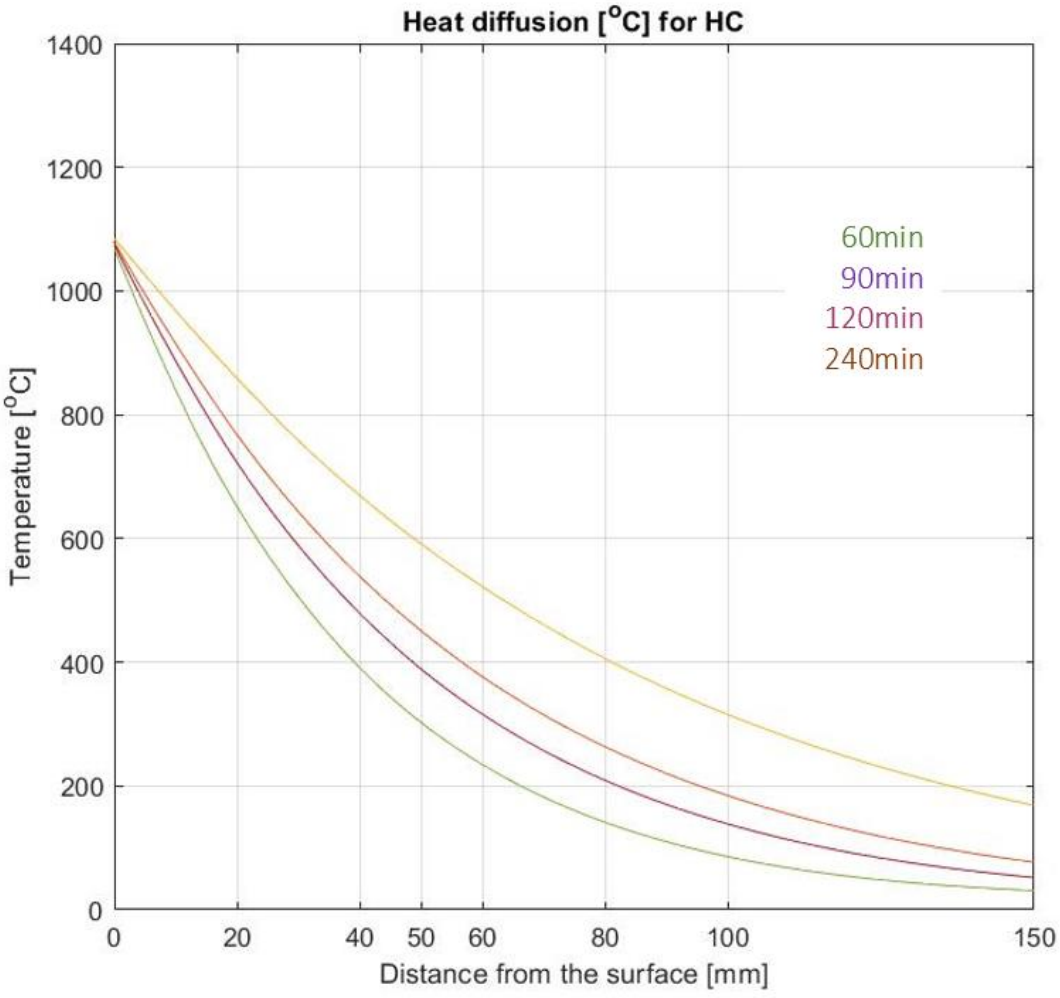

Figure 12-25 Heat diffusion for the HC fire curve, 1D model

The heat diffusion at selected distances from the surface is presented in the table 12-18 below. The values are an approximation.

Table 12-18 Heat diffusion at selected depths for the HC fire curve, 1D model

Distance from surface	HC, ANSYS 1D			
	60 min	90 min	120 min	240 min
0 mm	1069°C	1075°C	1079°C	1085°C
20 mm	650°C	725°C	770°C	860°C
40 mm	390°C	480°C	540°C	670°C
50 mm	305°C	390°C	450°C	590°C
60 mm	235°C	315°C	375°C	520°C
80 mm	140°C	210°C	265°C	405°C
100mm	85°C	140°C	185°C	315°C

13.Discussion

The discussion is based on the knowledge enhanced from the literature study, the knowledge obtained during meetings with experts, and the results obtained from the analyses performed in ANSYS.

13.1. Method

The method for understanding how fire should be modeled in the software started as a literature study where books, articles online, and tutorials online were investigated. In retrospect, this was not the preferred method to gain this understanding. The limitations of the student's version of ANSYS should probably also be considered at an earlier stage. An available software without these limitations could have been evaluated. This was probably forgotten because Bane NOR preferred the use of ANSYS and the use of a 3D model.

During the comparison, it is important to remember that the values given in the tables are an approximation. Because the temperature profiles from the literature study are not given in table form, this had to be performed manually by reading of the axes. The results obtained from ANSYS 1D-model are also an approximation but are taken as exact values and then rounded to the nearest 5°C. It was considered to use exact values for these analyses but because all the other values were an approximation this decision was taken.

The analyses are based on models only consisting of concrete. As argued in the theory chapter this is the normal approach. Since the reinforcing steel is placed parallel to the fire-exposed surfaces, it is assumed that the thermal conductivity of the steel is neglectable. The thermal calculations are also often performed to ensure that the reinforcing steel do not exceed certain temperatures, which makes the heat diffusion within the concrete more interesting.

13.2. 3D analyses vs. 1D analyses

Because Bane NOR preferred the use of the software ANSYS and the use of a 3D model, this was the basis for the study. The 3D analyses performed in ANSYS only considers heat transfer by conduction. As the theory stated, it is important that the heat transfer of all three forms are included in the analysis for heat diffusion. During these analyses, the fire curves were not considered to be gas-temperature curves as they are supposed to be. This was verified through the analyses where the maximum temperature was placed on the surface for the analyses. As can be seen in the result chapter (table 12-11 and 12-12) the values for both applying the fire curve as a direct load on the inner surface and for applying the maximum temperature for the fire duration as a direct load on the inner surface, gave exactly the same heat diffusion. This method is, therefore, not suited for comparing heat diffusion through concrete for different fire curves.

The 3D model could probably be modified to include both convection and radiation, but because of the limitations for the student's version of ANSYS, this would be a problem. As stated in the theory chapter, only 32 thousand nodes/elements can be defined in the student's version of ANSYS.

The mesh for the 3D model was not very fine for this type of analysis, with the finest obtained mesh of 0.15m. The mesh was also modelled irregular to obtain a finer mesh at the analysis point but were not adequate.

To dimension the heat transfer as a one-dimensional heat transfer through the concrete was therefore chosen. This was also a method that emerged through the preliminary project performed in advance of this study. This model allowed a much finer mesh, 0.002m. In these analyses, all the three forms of heat transfer were considered, and as will be discussed in sub-chapter 13.4 the results for the ISO 834 fire curve are comparable to the temperature profiles in the Eurocode 2.

13.3. Literature

Because the difficulty of finding relevant research the selection of articles for comparison is limited. This is a weakness of the study but also a finding of itself. There is not much available research on the topic.

13.3.1. ISO 834 fire curve

Table 13-1 ISO 834 fire curve: Eurocode 2 vs. research performed by Maraveas and Vrakas

ISO 834				
Distance from surface [mm]	**Eurocode 2**	**Eurocode 2**	**Maraveas and vrakas**	**Maraveas and vrakas**
	60min	**120 min**	**60 min**	**120 min**
0 mm	890°C	1010°C	800°C	1000°C
20 mm	510°C	690°C	600°C	750°C
40 mm	300°C	460°C	400°C	600°C

The table 13-1 above presents the temperature values for selected depths for the ISO 834 fire curve from both the Eurocode 2 and research performed by Maraveas and Vrakas. The values differ by the smallest of 10°C at the surface after 120 minutes and the largest at 40 mm distance with 140°C for the same time duration.

The difficulty by comparing the results is that the material properties for the analysis are different, which can be seen in the results. The Eurocode use a convection coefficient of 25 W/m^2K, while Maraveas and Vrakas use 50 W/m^2K on the exposed surface and 9 W/m^2K on the unexposed side. The Eurocode uses 1.5% moisture content as a parameter for the temperature profiles, while Maraveas and Vrakas use 3% of moisture content. The specific heat of concrete in the Eurocode is also defined varying with temperature as illustrated in chapter 12.2.1. Maraveas and Vrakas have also included the steel reinforcing in their analysis. Nevertheless, this reinforcement is placed at a depth of 45 mm and should not affect the heat diffusion before this.

13.3.2. RABT/ZTV fire curve

Table 13-2 RABT/ZTV fire curve: Research performed by Qiao et al. vs. Maraveas and Vrakas

RABT/ZTV		
Distance from surface [mm]	**Qiao et al.**	**Maraveas and Vrakas**
	60 min	**60 min**
0 mm	1200°C	1100°C
50 mm	600°C	800°C
100 mm	220°C	500°C

Because Qiao et al. and Maraveas and Vrakas did not use the same holding stage for the RABT/ZTV fire curve, there are very few results to compare. The results after 60 minutes will still be possible to compare. As shown in the table 13-2 above, the results do not correspond. In fact, Qiao et al. have obtained the gas-temperature on the surface of the section. This might be because they have placed the load directly at the inner surface, and thereby lost the convective and radiative heat transfer process at the surface. This is reminiscent of the method for placing the fire load used in the 3D model in ANSYS, which occurred to be inadequate for fire simulations.

Nevertheless, Qiao et al. obtain a lower temperature than Maraveas and Vrakas at 50 mm and 100 mm from the surface. Maraveas and Vrakas have as mentioned earlier, included steel reinforcement in their analysis, while Qiao et al. have not. They also have different values for multiple material properties, such as the concrete density, heat capacity coefficient, and the heat transfer coefficient.

13.3.3. RWS and HC

For the RWS fire curve, the research performed by Maraveas and Vrakas and the research by Boström and Larsen were investigated. The problem by comparing these two research articles is that they have not looked at the same distance from the surface. At 10 mm depth, after 120 minutes, Boström and Larsen achieved a temperature of 1000°C, while Maraveas and Vrakas achieved almost 1200°C at the concrete surface. Nevertheless, Maraveas and Vrakas performed a finite element analysis, while the research of Boström and Larsen were based on experimental testing.

For the HC fire curve, the only investigated research is the research performed by Maraveas and Vrakas, and no comparison is possible. Anyhow, there is a reason to believe that also this fire curve would experience different results if more data were available.

13.4. Comparison of Eurocode 2 and ANSYS

Because the results from the Eurocode 2 and the available research is not comparable, results obtained from the finite element analysis performed in ANSYS are mainly compared to each other. The results from the finite element analysis for the ISO 834 fire curve are anyhow compared to the temperature profiles presented in the Eurocode 2. Because the Eurocode is so well used and recognized internationally, these results are assumed to be the more correct to compare against. The material properties in the finite element analysis are also based on the properties presented in Eurocode 2.

13.4.1. ISO 834

Table 13-3 ISO 834: Comparison of the Eurocode 2 and ANSYS, 1D model

ISO 834		
Distance from surface	**EUROCODE 2**	**ANSYS**
	60 min	**60 min**
0 mm	890°C	900°C
20 mm	510°C	530°C
40 mm	300°C	315°C
50 mm	220°C	240°C
60 mm	180°C	190°C
80 mm	100°C	115°C
100mm	60°C	70°C

For comparison, a fire duration of 60 minutes is presented in the table 13-3 above. The results are very similar were the results from the analyses performed in ANSYS gives slightly higher temperatures. This is also the case if comparing other time durations. This corresponds well with the fact that the analyses in ANSYS is based on a moisture content of 0%, which makes the heat diffusion conservative compared to higher moisture contents. Additionally, it is important to remember that the values given in the tables are an approximation. The results from the analyses in ANSYS are rounded to the nearest 5°C, while the temperatures from the Eurocode are read of the temperature profiles. These results are close enough to conclude that the material model in ANSYS is adequate for further analyses and comparisons.

13.5. Comparison ANSYS

The material model in the software is as stated earlier based on values from the Eurocode 2. What is important to remember is that the convection coefficient α_c is not available for other fire curves than ISO 834 and the HC fire curve. The difference in the coefficient for these two curves are quite large, respectively 25 W/m^{2}K for the ISO 834 fire curve and 50 W/m^{2}K for the HC fire curve. In addition, the HC fire curve is more similar to the EUREKA and RWS fire curve, with a steeper heating curve and higher achieved temperatures. The convection coefficient for the HC fire curve are decided to be also used for the EUREKA and RWS fire curves. Whether or not this is the correct way is difficult to decide, but in lack of a better approach to the problem, this was decided.

Because Bane NOR experienced that some consultants ignored the recommendation of the EUREKA fire curve, and instead of using the recommended EUREKA 120 fire curve used the ISO 834 fire curve with a prolonged fire duration this scenario was investigated specifically.

13.5.1. ISO 834 240 min vs. EUREKA 120

When comparing the ISO 834 fire curve with a fire duration of 240 minutes to the EUREKA 120 fire curve, the temperatures seem to correspond. The highest temperatures obtained by the ISO 834 fire curve, except at the concrete surface where the EUREKA 120 fire curve achieves the highest temperature. This can be seen in the table 13-4 below.

Table 13-4 Comparison of ISO 834 (240min) and the EUREKA 120 fire curve, 1D model

Distance from surface	ISO 834	EUREKA 120	EUREKA 120
	240 min	120 minutes	240 min
0 mm	1140°C	1181°C	160°C
20 mm	870°C	835°C	290°C
40 mm	660°C	575°C	365°C
50 mm	575°C	480°C	380°C
60 mm	505°C	400°C	375°C
80 mm	385°C	280°C	340°C
100mm	295°C	195°C	290°C

Because EUREKA 120 is defined by a cooling stage that reaches 15°C after 230 minutes, the EUREKA 120 with a time duration of 240 minutes should also be considered. The cooling stage influences the heat diffusion and as can be seen in the table 13-4 the temperatures at 80 mm and 100 mm actually is higher after 240 minutes, than after 120 minutes, for the EUREKA 120 fire curve.

The temperatures are still lower than the ISO 834, but the values are very similar, and the values are also very close to the critical value of the concrete. The critical value of concrete is as stated in the theory chapter 300°C. Anyhow, according to table 8-1 in the theory chapter the steel reinforcing obtains full stress-strain relationship at this value (still 100% at 400°C).

At 60 mm the maximum temperature for the EUREKA 120 fire curve will be 400°C, and for the ISO 834 with a fire duration of 240 minutes, the temperature will be 505°C, which according to the table 8-1 in the theory chapter only gives 78% remained stress-strain relationship for the reinforcing steel.

This indicates that the ISO 834 fire curve with a prolonged fire duration instead of the EUREKA 120 fire curve is safe to use when fire calculations are performed. At the same time, it is indicated that this fire curve would simulate higher temperatures within the concrete. If the EUREKA 120 fire curve is adequate this could lead to an over-dimensioning, which is not cost-beneficial.

13.5.2. Concrete coverage

As stated in the theory chapter the critical value of concrete is 300°C, where the dehydration of the cement will lead to a significant decrease in the materials stiffness and strength. This will be an important factor when it comes to the rebuilding after a fire but as stated in the theory chapter structural failure normally only occurs when the reinforcing steel achieves a temperature that results in strength loss. Therefore, the achieved temperature within the reinforcing steel is the most used critical temperature value. In the theory chapter it is stated that the recommendation is that the reinforcing steel is not to be exceeding a temperature of 200-300°C because of the chance of exhibiting blue brittleness. However, this do not correspond with table 8-1 in the theory chapter where the critical value for the reinforcing steel is 400°C. The table is obtained from the Eurocode and is therefore followed in Norway, and also in this further discussion.

If the temperature of the reinforcing steel is not to be exceeding 400°C, the different fire curves will need a main coverage of the reinforcing steel as presented in the table 13-5 below, where the temperatures higher than 400°C are marked red.

Because the intention is to compare the maximum temperatures achieved in the concrete, the time duration of the analyses cannot be set to the same time. The EUREKA fire curve is the only curve with a cooling stage defined, and the temperatures will, therefore, decrease with a high time duration. The time of the fire duration is set to be 240 minutes for the ISO 834, HC and RWS fire curves. Results from EUREKA 60 and EUREKA 90 are presented in table 12-14 and 12-15 in the result chapter. The temperatures for these fire curves will achieve a smaller heat diffusion because the holding stage is shorter than for the EUREKA 120. As can be seen from these two tables and table 11-16 in the result chapter, the maximum temperatures are achieved at the same time as the holding stage finished. For the EUREKA 120 fire curve, the heat diffusion after 60 minutes is similar to the maximum temperatures for the EUREKA 60 fire curve. The same can be seen for the EUREKA 90 fire curve. The duration of fire is decisive for the heat diffusion and the defined cooling stage for these fire curves will be of significant importance for the results. Because of this, the EUREKA scenario is presented by the EUREKA 120 fire curve, which is the severest EUREKA scenario. The EUREKA 120 are presented for both a time duration of 120 minutes and 240 minutes because of the influence of the cooling period. The temperatures obtained at different depths are presented in the table 13-5 below.

Table 13-5 Comparison heat diffusion selected fire curves, 1D model

Distance from surface	ISO 834	EUREKA 120	EUREKA 120	HC	RWS
	240 min	120 minutes	240 min	240 min	240 min
0 mm	1140°C	1181°C	160°C	1085°C	1190°C
20 mm	870°C	835°C	290°C	860°C	940°C
40 mm	660°C	575°C	365°C	670°C	730°C
50 mm	575°C	480°C	380°C	590°C	645°C
60 mm	505°C	400°C	375°C	520°C	570°C
80 mm	385°C	280°C	340°C	405°C	440°C
100mm	295°C	195°C	290°C	315°C	340°C

If the temperature is not to be exceeding a temperature of 400°C at the reinforcing steel the coverage has to be set to at least 60 mm for the EUREKA 120 fire curve as can be seen in table 13-5 above. For the ISO 834 fire curve with a fire duration of 240 minutes, the main coverage seems to become 80 mm. For both the HC fire curve and the RWS fire curve the coverage to the reinforcing steel seems to be above 80 mm. Anyhow, the structures these fire curves are likely to be used for are normally dimensioned for a fire duration of 60 and 120 minutes. If the HC fire curve had a fire duration of 60 minutes, 40 mm of coverage would last. For the RWS fire curve, which normally would be dimensioned for a fire duration of 120minutes, the coverage will have to be over 60 mm because the temperature at this depth is 425°C. Because the temperature is very close to 400°C, and that the strength and stiffness of the reinforcing steel at 500°C still is 78%, a coverage of approximately 60 mm would probably still be adequate.

13.6. Effect of spalling

As it emerged from the literature study, the effect of spalling must be encountered when performing fire calculations for the calculations to be as accurate as possible. The addition of the polypropylene fibers will only reduce the chance of spalling not eliminating the risk. The known literature also states that the calculations should consider that some of the material is lost due to spalling but also addresses that this is difficult because there is not a method for estimating the amount of spalled material.

During this study, the possibility of spalling has been neglected by assuming an addition of polypropylene fibers in the concrete mixture. It is important to remember that these analyzes only are valid if this is fulfilled and that there does not occur any spalling. If spalling occurs a different heat diffusion inside the concrete would appear because of the reduction in the cross-section.

14. Conclusion

From the literature study, it emerges that there is little available research on heat diffusion for the fire curves and that the available research does not use the same parameters or framework for the analyses. This makes the research inadequate for comparison.

From the study regarding modelling fire in the software ANSYS, it emerged that the student's version has limitations of interest. Because of this, the mesh for a 3D-model would be coarse. It also emerged the importance of applying the fire load as a gas-temperature load and not as a temperature load on the surface area. The importance of including all three stages of heat transfer occurred during the literature study and also through the modelling in ANSYS. The preferred modelling method performed in this study is, therefore, a 1D-model based on elements with properties for radiation, convection, and conduction. In this model, the fire curves were applied as a gas-temperature curve on a space node located 2 mm from the surface of the concrete. To be able to compare the results to the Eurocode 2, the material parameters were based on the parameters given in the Eurocode. The results from this model corresponded well with the temperature profiles presented in Eurocode 2, which indicates that this was an adequate model for this kind of fire simulations.

What emerges from this study is that the different fire curves influence the heat diffusion in the concrete by the maximum achieved temperature, the steepness of the curve, the duration of the fire and the cooling stage. The fire curve with the largest heat diffusion in the concrete is the RWS fire curve, as assumed in advance. The EUREKA fire curve is the only curve with a cooling stage and is very dependent on how long the holding stage is. When comparing the EUREKA 120 fire curve to the ISO 834 fire curve with a fire duration of 240 minutes, the results from the analyses imply that the heat diffusion in the concrete would be higher for the ISO 834 fire curve.

The influence of concrete spalling during a fire is, however, neglected in the fire simulations performed in this study. It is important to remember that the rate of temperature rise influences the chance of spalling. This indicates that the choice of fire curve would influence the prediction of the amount of spalled concrete if concrete spalling is considered.

15. Recommendations

During a presentation by a representant from a fire product company, it was stated that the doors and ducts inside a tunnel are not designed for a fire curve different from the requirements in the standards. Which means that even if the structure is designed to withstand fire under a different fire scenario, the doors and ducts might not satisfy these requirements. For this study, evolving around the structural fire resistance of the tunnel and its resistance towards collapse, this would probably not influence. It would, however, be interesting to investigate this when it comes to human safety during the rescue.

In accordance with the Eurocodes guidelines, it would be interesting to also perform a structural analysis with the results from the thermal analyses to investigate the effect of how the fire affected concrete would influence the structural resistance of the structure. This should be performed before any assumptions regarding structural resistance are made. If there were more time in this study, this would have been performed.

It would also be interesting to investigate more concerning concrete spalling and the addition of polypropylene fibers. As the theory stated, the amount of spalled concrete is influenced by the heating rate, and it would, therefore, be interesting to investigate if the amount of added polypropylene fibers would be adequate regardless of choice of fire curve.

16. References

[1] Bygg21, "Industrialisering av byggeprosjekter," Available: https://www.bygg21.no/rapporter-og-veiledere/industrialisering-av-byggeprosjekter/

[2] A. Moum, H. Høilund-Kaupang, N. Olsson, and M. Bredeli, "Industrialisering av byggeprosessene. Status og trender," 2017.

[3] Bygg21, "Tenk nytt -Bruk kjente løsninger," Available: https://www.bygg21.no/rapporter-og-veiledere/tenk-nytt-bruk-kjente-losninger/

[4] M. K. Thompson and J. M. Thompson, *ANSYS mechanical APDL for finite element analysis*. Butterworth-Heinemann, 2017.

[5] Store Norske Leksikon. (2018). *Tunnel* [ONLINE]. Available: https://snl.no/tunnel

[6] T. F. Vegge. (10.11.18). *Vet ennå ikke om E 18 stenges i natt* [Online]. Available: https://www.fvn.no/nyheter/lokalt/i/Jd6xX/Vet-enna-ikke-om-E-18-stenges-i-natt

[7] P. Fiskerstrand. (2016). *Trøde-Bråhei tunnel*. Available: https://no.wikipedia.org/wiki/Tr%C3%B8de-Br%C3%A5hei_tunnel

[8] A. H. Buchanan and A. K. Abu, *Structural design for fire safety*. John Wiley & Sons, 2017.

[9] R. Qiao, Z. Shao, W. Wei, and Y. Zhang, "Theoretical investigation into the thermo-mechanical behaviours of tunnel lining during RABT fire development," pp. 1-12, 2018.

[10] C. Maraveas and A. Vrakas, "Design of concrete tunnel linings for fire safety," vol. 24, no. 3, pp. 319-329, 2014.

[11] L. Boström and C. K. Larsen, "Concrete for tunnel linings exposed to severe fire exposure," vol. 42, no. 4, pp. 351-362, 2006.

[12] K. Savov, R. Lackner, and H. Mang, "Stability assessment of shallow tunnels subjected to fire load," vol. 40, no. 8, pp. 745-763, 2005.

[13] H. Ingason and A. Lönnermark, "Recent achievements regarding measuring of time-heat and time-temperature development in tunnels," in *1st International Symposium on Safe & Reliable Tunnels, Prague, Czech Republic*, 2004, pp. 4-6.

[14] *Design of concrete structures part 1-2: General rules structural fire design*, NS-EN 1992-1-2:2004+NA:2010, 2004.

[15] I. A. Fletcher, S. Welch, J. L. Torero, R. O. Carvel, and A. Usmani, "The behaviour of concrete structures in fire," 2007.

[16] F. P. Incropera, A. S. Lavine, T. L. Bergman, and D. P. DeWitt, *Fundamentals of heat and mass transfer*. John Wiley & Sons, 2007.

[17] S.-H. Chang, S.-W. Choi, and J. Lee, "Determination of the combined heat transfer coefficient to simulate the fire-induced damage of a concrete tunnel lining under a severe fire condition," vol. 54, pp. 1-12, 2016.

[18] S.-W. Choi, J. Lee, and S.-H. Chang, "A holistic numerical approach to simulating the thermal and mechanical behaviour of a tunnel lining subject to fire," vol. 35, pp. 122-134, 2013.

[19] R. T. Tenchev, L. Li, and J. Purkiss, "Finite element analysis of coupled heat and moisture transfer in concrete subjected to fire," vol. 39, no. 7, pp. 685-710, 2001.

[20] B. Schrefler, P. Brunello, D. Gawin, and C. Majorana, "Concrete at high temperature with application to tunnel fire," vol. 29, no. 1, pp. 43-51, 2002.

[21] Simscale. (2017). *What is heat transfer* Available: https://www.simscale.com/docs/content/simwiki/heattransfer/whatisht.html

[22] Encyclopaedia Britannica. (2019). *Convection*. Available: https://www.britannica.com/science/convection

[23] *Actions on structures part 1-2:general actions, Actions on structures exposed to fire*, NS-EN 1991-1-2:2002+NA:2008, 2002.

[24] I. Asadi, P. Shafigh, Z. F. B. A. Hassan, and N. B. Mahyuddin, "Thermal conductivity of concrete – A review," *Journal of Building Engineering,* vol. 20, pp. 81-93, 2018.

[25] Encyclopaedia Britannica. (2015). *Thermal conduction* Available: https://www.britannica.com/science/thermal-conduction
[26] Encyclopaedia Britannica. (2018). *Thermal radiation* Available: https://www.britannica.com/science/thermal-radiation
[27] Encyclopaedia Britannica. (2018). *Stefan-Boltzmann law*. Available: https://www.britannica.com/science/Stefan-Boltzmann-law
[28] H. Ingason, Y. Z. Li, and A. Lönnermark, *Tunnel fire dynamics*. Springer, 2014.
[29] Promat. (2019). *Types of fire exposure* [Online]. Available: https://www.promat-tunnel.com/en/advices/fire-protection/fire%20curves
[30] A. d. Lange, "Fire design of load bearing concrete tunnels " Preliminary report Engineering sciences University of agder 2018.
[31] *Vegtunneler*, Håndbok N500, 2016.
[32] G. A. Khoury, "Effect of fire on concrete and concrete structures," vol. 2, no. 4, pp. 429-447, 2000.
[33] *Bruprosjektering*, N400, 2015.
[34] Autodesk. *Introduction to Autodesk Algor Simulation FEA* [ONLINE]. Available: http://download.autodesk.com/us/algor/userguides/mergedProjects/getting_started/Introduction_to_Algor/Introduction_to_Algor.htm
[35] ANSYS Inc. (2019). *ANSYS Free Student Software Downloads* [ONLINE]. Available: https://www.ansys.com/academic/free-student-products
[36] *ANSYS Mechanical APDL Basic Analysis Guide*, 2013.
[37] The MathWorks Inc. *What is MATLAB?* Available: https://se.mathworks.com/discovery/what-is-matlab.html?s_tid=srchtitle
[38] Bane NOR, "Veileder tunnelsikkerhet," 2018, Available: https://prosjekteringsveileder.jbv.no/wiki/veiledere/tunnelsikkerhet.
[39] *Design of concrete structures part 1-1: General rules and rules for buildings*, NS-EN 1992-1-1:2004+A1:2014+NA:2018, 2004.
[40] ANSYS Inc. (2019). *SOLID278 Element Description* [ONLINE]. Available: https://ansyshelp.ansys.com/account/secured?returnurl=/Views/Secured/corp/v192/ans_elem/Hlp_E_SOLID278.html
[41] ANSYS Inc. (2019). *Material reference* [ONLINE]. Available: https://ansyshelp.ansys.com/account/secured?returnurl=/Views/Secured/corp/v192/ans_mat/ans_mat.html
[42] ANSYS Inc. (2019). *LINK31 Element Description* Available: https://ansyshelp.ansys.com/account/secured?returnurl=/Views/Secured/corp/v192/ans_elem/Hlp_E_LINK31.html
[43] ANSYS Inc. (2019). *LINK33 Element Description* Available: https://ansyshelp.ansys.com/account/secured?returnurl=/Views/Secured/corp/v192/ans_elem/Hlp_E_LINK33.html
[44] ANSYS Inc. (2019). *LINK34 Element Description* Available: https://ansyshelp.ansys.com/account/secured?returnurl=/Views/Secured/corp/v192/ans_elem/Hlp_E_LINK34.html

17. Attachments

17.1. Supervision

17.2. Meetings